The Relationship Between Maturation Size and Maximum Tree Size From Tropical to Boreal Climates

(Article begins on next page)

31 January 2025

The Relationship between Maturation Size and Maximum Tree Size from Tropical to Boreal Climates

—

Valentin Journé,[1,2] Michał Bogdziewicz,[2] Benoit Courbaud,[1] Georges Kunstler,[1] Tong Qiu,[3] Marie-Claire Aravena Acuña,[4] Davide Ascoli,[5] Yves Bergeron,[6] Daniel Berveiller,[7] Thomas Boivin,[8] Raul Bonal,[9] Thomas Caignard,[10] Maxime Cailleret,[11] Rafael Calama,[12] J. Julio Camarero,[13] Chia-Hao Chang-Yang,[14] Jerome Chave,[15] Francesco Chianucci,[16] Thomas Curt,[17] Andrea Cutini,[18] Adrian Das,[19] Evangelia Daskalakou,[20] Hendrik Davi,[8] Nicolas Delpierre,[7] Sylvain Delzon,[10] Michael Dietze,[21] Sergio Donoso Calderon,[22] Laurent Dormont,[23] Josep Maria Espelta,[24] William Farfan-Rios,[25] Michael Fenner,[26] Jerry Franklin,[27] Catherine Gehring,[28] Gregory Gilbert,[29] Georg Gratzer,[30] Cathryn H. Greenberg,[31] Arthur Guignabert,[32] Qinfeng Guo,[33] Andrew Hacket-Pain,[34] Arndt Hampe,[35] Qingmin Han,[36] Mick E. Hanley,[37] Janneke Hille Ris Lambers,[38] Jan Holík,[39] Kazuhiko Hoshizaki,[40] Ines Ibanez,[41] Jill F. Johnstone,[42] Johannes M. H. Knops,[43] Richard K. Kobe,[44] Hiroko Kurokawa,[45] Jonathan Lageard,[46] Jalene LaMontagne,[47] Mateusz Ledwon,[48] François Lefèvre,[8] Theodor Leininger,[49] Jean-Marc Limousin,[50] James Lutz,[51] Diana Macias,[52] Anders Mårell,[53] Eliot McIntire,[54] Emily V. Moran,[55] Renzo Motta,[5] Jonathan Myers,[56] Thomas A. Nagel,[57] Shoji Naoe,[58] Mahoko Noguchi,[58] Julian Norghauer,[59] Michio Oguro,[45] Jean-Marc Ourcival,[50] Robert Parmenter,[60] Ian Pearse,[61] Ignacio M. Pérez-Ramos,[62] Łukasz Piechnik,[63] Tomasz Podgórski,[64] John Poulsen,[65] Miranda D. Redmond,[66] Chantal D. Reid,[67] Pavel Samonil,[39] C. Lane Scher,[67] William H Schlesinger,[67] Barbara Seget,[63] Shubhi Sharma,[68] Mitsue Shibata,[45] Miles Silman,[69] Michael Steele,[70] Nathan Stephenson,[19] Jacob Straub,[71] Samantha Sutton,[67] Jennifer J. Swenson,[72] Margaret Swift,[67] Peter A. Thomas,[73] Maria Uriarte,[74] Giorgio Vacchiano,[75] Amy Whipple,[76] Thomas Whitham,[76] S. Joseph Wright,[77] Kai Zhu,[78] Jess Zimmerman,[79] Magdalena Żywiec,[63] James S. Clark,[1,67]

[1] Universite Grenoble Alpes, Institut National de Recherche pour Agriculture, Alimentation et Environnement (INRAE), Laboratoire EcoSystemes et Societes En Montagne (LESSEM), 38402 St. Martin-d'Heres, France.
[2] Forest Biology Center, institute of environmental biology, Adam Mickiewicz University in Poznan, Poland.
[3] Department of Ecosystem Science and Management, Pennsylvania State University, University Park, PA 16802 USA.
[4] Centro Austral de Investigaciones Científicas (CADIC), Consejo Nacional de Investigaciones Científicas y Técnicas (CONICET), B. Houssay 200 (9410) Ushuaia, Tierra del Fuego, Argentina.
[5] Department of Agriculture, Forest and Food Sciences, University of Torino, 10095 Grugliasco, TO, Italy.

1

[6]Forest Research Institute, University of Quebec in Abitibi-Temiscamingue, Rouyn-Noranda, QC J9X 5E4, Canada.

[7]Université Paris-Saclay, CNRS, AgroParisTech, Ecologie Systématique et Evolution, 91190, Gif-sur-Yvette, France.

[8]Institut National de Recherche pour Agriculture, Alimentation et Environnement (INRAE), Ecologie des Forets Mediterranennes, 84000 Avignon, France.

[9]Department of Biodiversity, Ecology and Evolution, Complutense University of Madrid, 28040 Madrid, Spain.

[10]Universite Bordeaux, Institut National de Recherche pour Agriculture, Alimentation et Environnement (IN-RAE), Biodiversity, Genes, and Communities (BIOGECO), 33615 Pessac, France.

[11]INRAE, Aix-Marseille University, UMR RECOVER, Aix-en-Provence, France.

[12]ICIFOR (Forest Research Institute). INIA-CSIC. 28040 Madrid. Spain.

[13]Instituto Pirenaico de Ecologla, Consejo Superior de Investigaciones Cientificas (IPE-CSIC), 50059 Zaragoza, Spain.

[14]Department of Biological Sciences, National Sun Yat-sen University, Kaohsiung 80424, Taiwan.

[15]Unité Evolution et Diversité Biologique (EDB), CNRS, IRD, UPS, 118 route de Narbonne, 30162 Toulouse, France.

[16]CREA - Research Ventre for Forestry and Wood, Viale S. Margherita 80, 52100 Arezzo, Italy.

[17]Aix Marseille universite, Institut National de Recherche pour Agriculture, Alimentation et Environnement (INRAE), 13182 Aix-en-Provence, France.

[18]Research Centre for Forestry and Wood, Arezzo, Italy.

[19]USGS Western Ecological Research Center, Three Rivers, CA, 93271 USA.

[20]Institute of Mediterranean and Forest Ecosystems, Hellenic Agricultural Organization, 11528 Athens, Greece.

[21]Earth and Environment, Boston University, Boston, MA, 02215 USA.

[22]Universidad de Chile, Facultad de Ciencias Forestales y de la Conservacion de la Naturaleza (FCFCN), La Pintana, 8820808 Santiago, Chile.

[23]Centre d'Ecologie Fonctionnelle et Evolutive (CEFE), Centre National de la Recherche Scientifique (CNRS), 34293 Montpellier, France.

[24]Centre de Recerca Ecologica i Aplicacions Forestals (CREAF), Bellaterra, Catalunya 08193, Spain.

[25]Biology Department, Center for Energy, Environment, and Sustainability, Wake Forest University, Winston Salem, NC, United States.

[26]Biology Department, University of Southampton, United Kingdom.

[27]Forest Resources, University of Washington, Seattle, WA 98195 USA.

[28]Department of Biological Sciences and Center for Adaptive Western Landscapes.

[29]Department of Environmental Studies, University of California, Santa Cruz, CA 95064 USA.

[30]Institute of Forest Ecology; Department of Forest- and Soil Sciences, University of Natural Resources and Life Sciences, Vienna.

[31]Bent Creek Experimental Forest, USDA Forest Service, Asheville, NC 28801 USA.

[32]INRAE, Bordeaux Sciences Agro, UMR 1391 ISPA, Villenave d'Ornon, France.

[33]Eastern Forest Environmental Threat Assessment Center, USDA Forest Service, Southern Research Station, Research Triangle Park, NC 27709 USA.

[34]Department of Geography and Planning, School of Environmental Sciences, University of Liverpool, Liver-

[75] pool, United Kingdom.

[35] BIOGECO, INRA, University of Bordeaux, Cestas, France.

[36] Department of Plant Ecology Forestry and Forest Products Research Institute (FFPRI), Tsukuba, Ibaraki, 305-8687 Japan.

[37] School of Biological and Marine Sciences, University of Plymouth, Plymouth, United Kingdom.

[38] Plant Ecology, Institute of Integrative Biology, D-USYS, ETH Zürich, Zürich, Switzerland.

[39] Department of Forest Ecology, Silva Tarouca Research Institute, 60200 Brno, Czech Republic.

[40] Department of Biological Environment, Akita Prefectural University, Akita 010-0195, Japan.

[41] School for Environment and Sustainability, University of Michigan, Ann Arbor, MI 48109.

[42] Institute of Arctic Biology, University of Alaska, Fairbanks, AK 99700, USA.

[43] Health and Environmental Sciences Department, Xian Jiaotong-Liverpool University, Suzhou, China, 215123.

[44] Department of Plant Biology, Program in Ecology, Evolutionary Biology, and Behavior, Michigan State University, East Lansing, MI 48824.

[45] Department of Forest vegetation, Forestry and Forest Products Research Institute, Tsukuba, Ibaraki, 305-8687, Japan.

[46] Department of Natural Sciences, Manchester Metropolitan University, Manchester M1 5GD, UK.

[47] Department of Biological Sciences, DePaul University, Chicago, IL 60614 USA.

[48] Institute of Systematics and Evolution of Animals, Polish Academy of Sciences, Slawkowska 17, 31-016 Krakow, Poland.

[49] USDA, Forest Service, Southern Research Station, PO Box 227, Stoneville, MS 38776.

[50] CEFE, Univ Montpellier, CNRS, EPHE, IRD, 1919 route de Mende, 34293 Montpellier Cedex 5, France.

[51] Department of Wildland Resources, and the Ecology Center, Utah State University, Logan, UT 84322 USA.

[52] Department of Biology, University of New Mexico, Albuquerque, NM 87131 USA.

[53] INRAE, UR EFNO, FR-45290 Nogent-sur-Vernisson, France.

[54] Pacific Forestry Centre, Victoria, British Columbia, V8Z 1M5 Canada.

[55] School of Natural Sciences, UC Merced, Merced, CA 95343 USA.

[56] Department of Biology, Washington University in St. Louis, St. Louis, MO.

[57] Department of forestry and renewable forest resources, Biotechnical Faculty, University of Ljubljana, Ljubljana, Slovenia.

[58] Tohoku Research Center, Forestry and Forest Products Research Institute, Morioka, Iwate, 020-0123, Japan.

[59] Institute of Plant Sciences, University of Bern, Altenbergrain 21, Bern 3013, Switzerland.

[60] Valles Caldera National Preserve, National Park Service, Jemez Springs, NM 87025 USA.

[61] Fort Collins Science Center, 2150 Centre Avenue, Bldg C, Fort Collins, CO 80526 USA.

[62] Inst. de Recursos Naturales y Agrobiologia de Sevilla, Consejo Superior de Investigaciones Cientificas (IRNAS-CSIC), Seville, Andalucia, Spain.

[63] W. Szafer Institute of Botany, Polish Academy of Sciences, Lubicz 46, 31-512 Krakow, Poland.

[64] Department of GameManagement and Wildlife Biology, Faculty of Forestry and Wood Sciences,Czech University of Life Sciences Prague; Kamýcká 129, 165 00 Prague, Czech Republic.

[65] The Nature Conservancy, Boulder, CO 80302.

[66] Department of Environmental Science Policy and Management, University of California Berkeley, Berkeley,

116 California, USA.

117 [67]Nicholas School of the Environment, Duke University, Durham, NC 27708 USA.

118 [68]Ecology and Evolutionary Biology Department, Yale University, 165 Prospect Street, New Haven, USA.

119 [69]Department of Biology, Wake Forest University, 1834 Wake Forest Rd, Winston-Salem, NC 27106 USA.

120 [70]Department of Biology, Wilkes University, 84 West South Street, Wilkes-Barre, PA 18766 USA.

121 [71]Department of Environmental Science and Ecology, State University of New York-Brockport, Brockport, NY

122 14420 USA.

123 [72]Data Science, College of William and Mary, Williamsburg, VA, USA.

124 [73]School of Life Sciences, Keele University, Staffordshire ST5 5BG, UK.

125 [74]Department of Ecology, Evolution and Environmental Biology, Columbia University, 1113 Schermerhorn

126 Ext., 1200 Amsterdam Ave., New York, NY 10027.

127 [75]Department of Agricultural and Environmental Sciences - Production, Territory, Agroenergy (DISAA), Uni-

128 versity of Milan, 20133 Milano, Italy.

129 [76]Department of Biological Sciences, Northern Arizona University, Flagstaff, AZ 86011 USA.

130 [77]Smithsonian Tropical Research Institute, Apartado 0843n03092, Balboa, Republic of Panama.

131 [78]School for Environment and Sustainability, University of Michigan, Ann Arbor, Michigan, USA.

132 [79]Department of Environmental Sciences, University of Puerto Rico, Rio Piedras, PR 00936 USA

133

The fundamental trade-off between current and future reproduction has long been considered to result in a tendency for species that can grow large to begin reproduction at a larger size. Due to the prolonged time required to reach maturity, estimates of tree maturation size remain very rare and we lack a global view on the generality and the shape of this trade-off. Using seed production from five continents, we estimate tree maturation sizes for 486 tree species spanning tropical to boreal climates. Results show that a species' maturation size increases with maximum size, but in a non-proportional way: the largest species begin reproduction at smaller sizes than would be expected if maturation were simply proportional to maximum size. Furthermore, the decrease in relative maturation size is steepest in cold climates. These findings on maturation size drivers are key to accurately represent forests' responses to disturbance and climate change.

keywords: tree fecundity | size | seed production | tree maturation | life-history | allometry

Running title:

Relation between Maturation and Maximum Tree Size

Data and code availability statement

Data and code supporting our results are archived on the Open Science Framework (OSF) Repository: https://doi.org/10.17605/OSF.IO/U23VY. All analyses used R Core Team (2023) (v4.3.0) and published R packages.

Author contributions

V.J., G.K. and J.S.C performed analyses, led the paper, and designed the study. V.J., M.B., B.C., G.K., T.Q, and J.S.C co-wrote the paper. J.S.C compiled the MASTIF network, and wrote the MASTIF model and software. All authors contributed data and revised the paper.

correspondence:

Journé Valentin*: journe.valentin@gmail.com & James S. Clark†: jimclark@duke.edu

*Forest Biology Center, institute of environmental biology, Adam Mickiewicz University in Poznan, Poland.

† Nicholas School of the Environment, Duke University, Durham, NC 27708 USA.

Introduction

The size or age at maturity is critical for tree population fitness and forest regeneration because recruitment opportunities can occur when trees are any size or age (Dietze & Clark, 2008; McDowell *et al.*, 2020; Qiu *et al.*, 2021). In trees, reproduction follows an extended maturation phase (Thomas, 1996; Clark *et al.*, 2004). Juvenile allocation to leaves and the roots and architecture that supports them build the large light- and water-harvesting capacity characteristic of the tree life form. Allocation can then shift to include reproduction. This delayed maturation of trees is linked to the fundamental trade-off between current and future reproduction (Stearns, 1989).

On one hand, delayed reproduction sacrifices early seed production to reap future benefits. In environments marked by intense competition and a reliable future, delayed reproduction benefits from large size and the resources that accumulate if juveniles allocate to growth and survival (Falster & Westoby, 2003; Wenk & Falster, 2015). On the other hand, the advantages of large size can come with costs, including water transport high into the crown and biomechanical risk of bole fracture or windthrow (Niklas, 1994; Koch *et al.*, 2004; Dietze & Clark, 2008; Lines *et al.*, 2012). Current reproduction avoids the risks of an uncertain future, and it contributes most to fitness in non-competitive or frequently disturbed environments (Charlesworth, 2000).

Among tree species, the potential trade-off between current and future reproduction might require a balance of benefits and risks and result in a positive association across species in maturation and maximum size or age (Loehle, 1988; Thomas, 1996; Davies & Ashton, 1999; Westoby *et al.*, 2002; Falster & Westoby, 2003; Wenk & Falster, 2015; Visser *et al.*, 2016). Our understanding of the variation of maturation size among tree species is, however, extremely limited and there are no large-scale studies on this topic. We thus have a poor understanding of how maturation size varies with species maximum size and the relative importance of other factors such as species climate niche and functional traits.

In the absence of maturation estimates, earth system models (ESMs) incorporate assumptions that are expected to bias lifetime reproduction. Many ESMs omit impacts of life history on disturbance response entirely (see McDowell *et al.* 2020 for a review). In models that do accommodate life history, maturation size $- d_{mat}$ (for diameter) $-$ is independent of maximum size $- d_{max}$ (Kohler & Huth, 2004; Wallentin *et al.*, 2008; Yang *et al.*, 2022) (Fig. 1, black dotted line). An alternative hypothesis is that maturation size is proportional to maximum size. It is consistent with a study at Barro Colorado Island in Panama, where Visser *et al.* (2016) reported that $d_{mat} = d_{max}/2$ (red dashed line in Fig. 1). This is related to the classical prediction of a proportionate increase in maturation age with increased maximum age from simple optimization models in animals (Charnov & Berrigan, 1990, 1991; Jensen, 1996; Thorson *et al.*, 2017) and trees (Clark, 1991). Indeed, if the predictions for age also apply to size, then this **proportionate risk model** means that the maturation delay incurred for increased maximum size is the same for species large and small, represented by the red line in Fig. 1.

In fact, it would be remarkable if this relationship was the same for species of all sizes because the constraints on the large size and the relative contribution to fitness of early seed production could vary widely depending on the species' maximum size. If mortality risks and allocation demands change with age and size (Charnov & Berrigan, 1990), then the strictly proportional relationship between maturation size (d_{mat}) and maximum size (d_{max}) can be generalized to a power relationship,

7

$$d_{mat} = \alpha \times d_{max}^{\beta_d} \tag{1}$$

The proportionate model means that $\beta_d = 1$ in Eq. (1) (Fig. 1a). An **accelerating risk model** refers to the case where the maturation delay required for large species to increase maximum size is greater than for small species. If $\beta_d > 1$ (purple in Fig. 1), the relative size at maturation ($d_{rel} = d_{mat}/d_{max}$) continues to increase for species in the largest size classes (Fig. 1b). Consider, for example, an expected fitness gain from extending end-of-life reproduction that comes with increased size and age. The early life investments in structural support or defenses needed for an incremental increase in maximum size might be especially high for the largest species.

Alternatively, a **diminishing risk model** refers to the case where the need to further delay maturation size declines for species already at large size. If $0 < \beta_d < 1$, then species that reach large size do not incur the same proportionate delay risk as small species. As β_d approaches zero, the largest species mature at nearly the same size as the small species. Then, the relative size at maturation d_{rel} declines with maximum size (Fig. 1b).

Improved understanding of maturation size confronts challenges posed by slow dynamics and limited observation. Where there is a dense canopy, the reproductive status of individual trees is often not detected, and crop failures (little or no seed production in trees that have reached maturity) are common. Likewise, seed traps often fail to recover seeds from nearby reproductive trees, especially the low seed production of newly mature individuals (LaDeau & Clark, 2001). Detection error can be minimized where observations come from above the canopy or open settings like savannas, seed orchards, or common gardens (LaDeau & Clark, 2001; Caignard *et al.*, 2021). Still, a time series of observations is needed because an individual reproducing this year will have matured at some time in the past. Estimates of maturation status from time series data allow for detection error similar to the way it is used in capture-recapture models. Maturation can be treated as a hidden Markov process (see detailed Supplements to Clark *et al.* 2004, 2019). As in capture-recapture models, the probability that an individual is mature in a given year depends not only on failure to detect in the current year but also on the history and future of observations on the same individual. The more times that reproduction is not detected in the past (or future), the lower the probability that a tree is mature now. In tree-fecundity studies, the complexity is compounded by the "masting" phenomenon, where quasi-synchronous, quasi-periodic crops require observations over several years, making a large number of observations in a single year insufficient. Most studies where maturation size has been estimated focus on open-grown trees and/or have limited taxonomic breadth, habitat variation, or both (Wenk *et al.*, 2018; Thomas, 1996; Davies & Ashton, 1999; Kohyama *et al.*, 2003; Wright *et al.*, 2005; Visser *et al.*, 2016; Minor & Kobe, 2019).

Inferring the relationship between maturation and maximum size has also to control for the environment (Wenk & Falster, 2015) and species characteristics (Visser *et al.*, 2016). While the effects of climate on maturation size are unknown, tree fecundity responds to seasonal temperature and moisture, soils, and light availability, which depends on the local competitive environment (Clark *et al.*, 2014; Caignard *et al.*, 2017; Minor & Kobe, 2019; Le Roncé *et al.*, 2021; Qiu *et al.*, 2022; Journé *et al.*, 2022). Also, fast growth and accelerated competition that comes from long growing seasons in the wet tropics do not necessarily imply small or large maturation sizes.
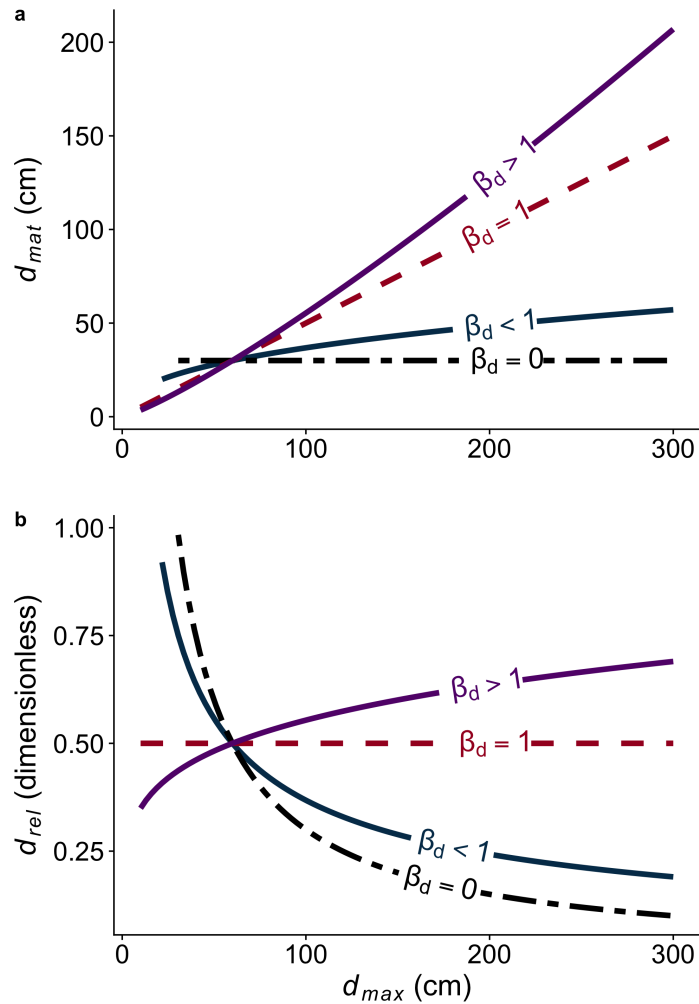
Figure 1: Hypothesized association between maturation size (d_{mat}) and maximum size (d_{max}) (**a**) and the relative size at maturation ($d_{rel} = d_{mat}/d_{max}$) (**b**) (Eq. (1)). To highlight the effects of size (parameter β_d), values of parameter α are selected to yield an equivalent diameter at $d_{max} = 60$ cm. Two "baseline" hypotheses (dashed lines) are independence between d_{mat} and d_{max} (black dotted) and proportionate delay (red dotted), the latter is expected if increased size incurs the same maturation delay at all size classes. Two alternative hypotheses are increasing (purple - accelerating risk model) or decreasing (blue - diminishing risk model) maturation delays in the largest size classes.

The relationship between maturation and maximum size could be associated with other plant functional traits, that would reflect diverse plant strategies. Fast growth in open environments is often associated with low wood density and high specific leaf area (SLA) (Moles *et al.*, 2004, 2006; Thomas *et al.*, 2015; Visser *et al.*, 2016; Wenk *et al.*, 2018). However, it is unclear whether the same traits that are involved in fast growth are also associated with maturation at a small size. Furthermore, if large-seeded species need to accumulate resource reserves, then there could be a positive association between seed size and maturation size (Moles *et al.*, 2004). Relatedly, high reproductive expenditures, measured as seed size × seed number (Qiu *et al.*, 2022), might be associated with delayed maturation size. Due to their co-dependence, it is necessary to model all of these traits jointly, while accounting for the effects of habitat and phylogenetic groups (Clark, 2016; Seyednasrollah & Clark, 2020; Bogdziewicz *et al.*, 2023; Qiu *et al.*, 2023).

In this study, we provide the first comprehensive estimates of tree maturation size, obtained for 486 tree species on five continents, incorporating effects of the environment over a large range of tree diameters and habitats. We use the Masting Inference and Forecasting (MASTIF) network and modeling framework to accommodate the dependence between observations between trees and within trees over time (Clark *et al.*, 2021; Sharma *et al.*, 2022; Qiu *et al.*, 2022; Journé *et al.*, 2022). Based on MASTIF estimates we derive maturation size as tree diameter at the onset of female reproductive function allowing us to compare maturation sizes across species that vary in reproductive biology (e.g., Pinaceae commonly produce male cones earlier than female cones; many species have no such separation) and where pollen production can be hard to quantify. We first evaluate how maturation varies with species' maximum size and test the three alternative models of Fig. 1 with our estimates of maturation size and estimates of species' maximum size. Then, we evaluate how the relationship between maturation size and maximum size is influenced by climate and its association with other plant functional traits.

Materials and Methods

Our analysis includes three elements (Fig. 2). We first parameterize a model for individual maturation status and fecundity based on diameter, shade conditions, and environmental variables (Fig. 2a). The year in which an individual achieves maturity is almost never observed. Instead, seeds counted in traps or in crowns vary from year to year. Successive observations represent a time series for every tree. This first step estimates maturation status and conditional fecundity (seeds per tree per year given that it is mature) for all trees in the network. From this fitted model, we generate predictive distributions of maturation status across diameter with other variables held at intermediate values to estimate d_{mat} from the model. Again, this prediction from the model is necessitated by the fact that true maturation status is an estimate, not a state that is directly observed. Second, we estimated the model of Fig. 1 to obtain estimates of α and β_d (Fig. 2b), while controlling for other variables that could affect their relationship. Finally, we evaluate the species-level trait relationship that includes maturation size (Fig. 2c). The following section describes these elements of the analysis.

10

a) Individual observations → Species' tree maturation size (d_mat)

Parameters: main effects, interaction, random individual & year
Latent variables: maturation status, conditional fecundity

Fitted MASTIF

crop counts (CC), seed traps (ST)

Species level prediction
tree maturation size (d_{mat})

b) Proportionate cost model

Parameters: α, β_d
Climate effects

c) Trait analysis

Fitted GJAM
tree maturation size
+ other traits
+ climate effects

Conditional prediction
trait relationships

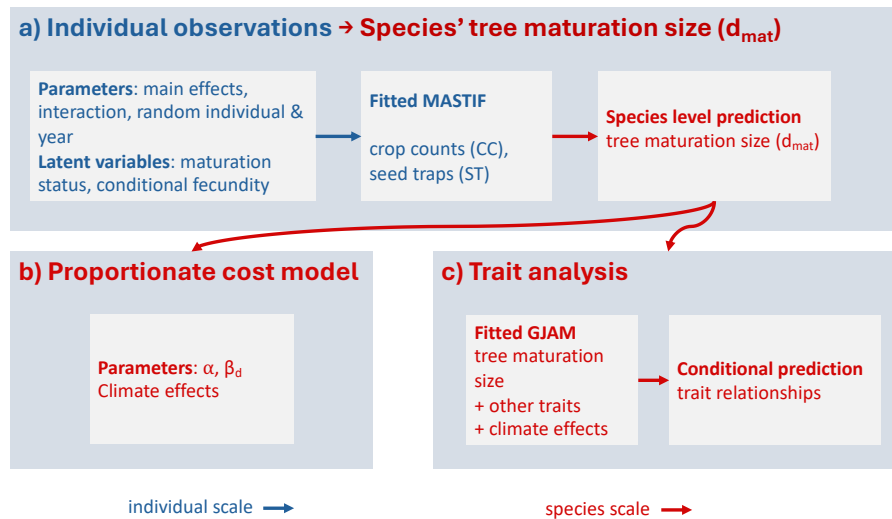individual scale →   species scale →

Figure 2: Three elements of the analysis include a) an individual-scale analysis (blue) to estimate maturation status each year and to parameterize relationships that control maturation. This fitted model is the basis for species-level prediction of maturation size (red). b) Species-level expected maturation size based on the proportionate risk model, controlling for species' differences in their climate domains. c) Analysis of species-level trait relationships with maturation size.

MASTIF data and model

The MASTIF model and data summarized here are detailed in Clark *et al.* (2019) and its extended Supplement (see also Qiu *et al.* 2021, 2022; Journé *et al.* 2022). Data are of two types, crop counts on trees and seed traps in mapped inventory plots (MASTIF) (Clark *et al.*, 2019) (Fig. S1). The initial sample size is approximately 12 million tree-years from five continents on 898 species and 112 families. The majority of observations (99%) are derived from longitudinal studies, involving repeated observations of all trees on a plot or individual trees. The remaining crop count observations (1%) are collected opportunistically through the iNaturalist project MASTIF (Clark *et al.*, 2019). The number of species observed per plot ranges from 1 to 221 species. The number of species observations is larger for seed trap monitoring (476 species in total, 22,929 tree-year observations on average) than for crop count monitoring (130 species in total, 1,058 tree-year observations on average). Most plots are localized in North America and central Europe (97%), whereas most species observations are coming from South America (54%). On average, 75% of individual tree year observation are coming from the tropics. Additional information is provided in Table S1 and Supplementary Files 1 and 2. For both data types, observations include species, diameter, shade class (ranging from "full sun", class 1, to "full shade", class 5), number of fruiting structures, and an estimate of the fraction of the total crop represented by the count. For crop counts, the data model is beta-binomial, with binomial uncertainty for the counts given crop fraction, and beta uncertainty for crop fraction. The seed traps data additionally include mapped locations of trees and seed traps, which is used to jointly estimate fecundity, dispersal, and, for seeds identified only to

11

genus, species identity. For seed traps, the data model is Poisson for counts given dispersal and species, a bivariate Student's t (i.e. 2Dt) redistribution kernel for dispersal (Clark *et al.*, 1999), and a multinomial species probability (many seeds are identified only to genus level).

The MASTIF model is a dynamic model for year-to-year and tree-to-tree seed production. The model allows for conditional independence in crop counts and seed traps data through latent states. It estimates maturation state and conditional fecundity (seed production given the individual is mature), which depend on tree size, shading, local climate, and soil conditions. Random effects on individuals and years allow for wide variation between trees and over time. The posterior distribution includes the parameters and latent states presented in Clark *et al.* (2019), and summarized in Qiu *et al.* (2022) and Journé *et al.* (2022). Model fitting was accomplished with Gibbs sampling, a Markov chain Monte Carlo technique based on sampling from conditional distributions. Model structure and methodology are implemented with the R package Mast Inference and Forecasting (`mastif`, v1.0.1) (Clark *et al.*, 2019).

Derivation of tree maturation size from fitted MASTIF model

Tree maturation size (d_{mat}) is derived from an individual-scale model fitted to each species with MASTIF. We define tree maturation size (d_{mat}) as the diameter when a tree is mature and has the capacity to produce enough seed to construct one fruiting structure, f_{min}. For species that produce one-seeded fruits (e.g., *Quercus, Juglandaceae*), $f_{min} = 1$. For species that produce cones (e.g., Pinaceae, Cupressaceae), pods (e.g., Fabaceae, Bignoniaceae), or other capsules that house multiple seeds (e.g., *Fagus* capsules), f_{min} is the number of seeds contained in that structure. The data and definitions we use to determine d_{mat} differ from those employed in previous studies (e.g. Visser *et al.* 2016), as we use both crop count and seed trap observation and not only maturation status. The estimation of individual fecundities, obtained through MASTIF model, is also included, taking into account tree characteristics and environment (Clark *et al.*, 2021; Qiu *et al.*, 2021; Journé *et al.*, 2022). MASTIF models the effects of environmental predictors on conditional fecundity (given mature status), because immature trees do not respond to predictors (it is always zero). [Modeling environmental effects on (unconditional) fecundity would make no more sense than including immature individuals in studies of masting intervals or synchronicity.] Conditional fecundity ψ is represented by a log-normal distribution, which allows for the effects of the environment. The log-normal is undefined for zero seeds. Zeros are accommodated by the fact that trees can be in the immature state ($\rho = 0$), or conditional fecundity can be below the threshold f_{min}, as in a failed seed crop (Clark *et al.*, 2004, 2019),

$$f = \begin{cases} \psi & \rho = 1 \\ 0 & (\rho = 0) + (\rho = 1)(\psi < f_{min}) \end{cases} \tag{2}$$

An individual is immature until the first time fecundity rises above the threshold for producing fruit, i.e., $(\rho_{i,t} = 1)(\psi_{i,t} > f_{min})$. Specifically for tree i in year t,

$$f_{i,t} = \psi_{i,t} \times \rho_{i,t}$$

$$\rho_{i,t}|\rho_{i,t-1}, \rho_{i,t+1} \sim Bernoulli\left(\rho_{i,t-1} + (1 - \rho_{i,t-1})\rho_{i,t+1}\Phi(\beta_0^\rho + \beta_1^\rho d_{i,t})\right)$$

$$\log \psi_{i,t} \sim N(\mathbf{x}'_{i,t}\boldsymbol{\beta}^x + \ldots, \sigma^2) \tag{3}$$

where $\Phi(\cdot)$ is the standard normal cumulative distribution function for the probit probability of transitioning to the mature state, depending on tree diameter $d_{i,t}$. Importantly, $\Phi(\beta_0^\rho + \beta_1^\rho d_{i,t})$ it is the probability of making the transition for an individual that is now in the immature state. For this reason, the coefficients $\beta_0^\rho, \beta_1^\rho$ for maturation in the second line of Eq. (3) engage only for the transition tree-years, $[\rho_{i,t}|\rho_{i,t-1} = 0, \rho_{i,t+1} = 1]$. Predictors in the design vector for conditional fecundity $\mathbf{x}'_{i,t}$ include the mean climate variables (defined at the species level) tested here and competition by neighbors, and $\boldsymbol{\beta}^x$ is the estimated parameter vector. The ellipses $(\ldots)$ in Eq. (3) includes individual effects (subscript i) and year effects (subscript t) (Clark *et al.*, 2019). The variance not assigned to predictors is $s^2 = \sigma^2 + Var(\text{individuals}) + Var(\text{years})$.

Setting all other fitted variables at their mean values and intermediate shade (shade class 3 on the scale from 1 to 5), we obtained (unconditional) fecundity f from the fitted model. We first factored the joint distribution of conditional fecundity and maturation,

$$[\psi > f_{min}, \rho = 1] = [\psi > f_{min}|\rho = 1][\rho = 1] \tag{4}$$

Using Bayes' theorem, the cumulative distribution function for maturation diameter is

$$[d_{matr} > d|\psi > f_{min}, \rho = 1] \propto [\psi > f_{min}, \rho = 1|d][d]$$
$$= [\psi > f_{min}|\rho = 1, d][\rho = 1][d]$$
$$= \Phi(z_1)\,\Phi(z_2)\,[d] \tag{5}$$

where $z_1 = \frac{\log f_{min} - \mathbf{x}'\boldsymbol{\beta}^\psi}{s}$ (log normal fecundity), $z_2 = \beta_0^\rho + \beta_0^\rho d$ (probit maturation), and again, s^2 is the marginal variance for conditional fecundity. We have taken the diameter distribution $[d]$ to be uniform. The distribution of maturation size is obtained using inverse distribution sampling from Eq. (5), and we estimated d_{mat} as the mean of this distribution. We selected species for which maturation and fecundity schedules could be estimated with confidence. The selection was based on estimates of maturation status from the MASTIF model, and we retained species with at least 10 immature and 10 mature individuals. This included 486 species observed over a range of values for diameters.

Trait and climate data

Like maximum tree height or age, maximum tree diameter is a useful concept, despite the fact that it cannot be known. To incorporate the concept of size differences, we use extreme sizes available from literature and our inventory data, recognizing that the concept of a maximum becomes most meaningful with large sample sizes, which are not available for all species. For the final analysis here, we kept the highest estimates

of d_{max}. Sources in Table S3 include tropical species from large plots in central Panama (189 species) and French Guyana (33 species), which together represent 45.7% of values. Estimates extracted from the internet (e.g. encyclopedia, online flora) include 173 species (35.6%) (Table S3). For species not estimated in other sources, we used forest inventory data, evaluated by two approaches, both based on order statistics. We avoided using the absolute largest reported value in forest/MASTIF inventories due to the high noise levels associated with extremes. Order statistics were preferred over quantiles, the latter being determined by whether there are huge numbers of small trees in the data set; quantiles are based on the entire stand structure, whereas here the goal is to estimate the largest sizes, regardless of whether there are few or many small trees. For species present in national forest inventories we estimated d_{max} following Qiu *et al.* (2021) by using the tenth largest order statistic (38 species, 7.8%). For the remaining species present in MASTIF inventories, and with at least more than 90 unique individuals, we used the fifth largest order statistics (representing in total 8.4%). For species having only maximal plant height (Liu *et al.*, 2019), but no d_{max}, we converted them to d_{max} using allometric equations of Feldpausch *et al.* (2011) (12 species, <2.5%). Observations of d_{max} coming from the internet are usually higher than data from National Forest Inventories, allometric predictions, and MASTIF inventories (Fig. S2). Seed size estimates came from measurements in our lab (Clark *et al.*, 2021), the primary literature, and the TRY Plant Trait Database (Kattge *et al.*, 2011). Wood density and SLA are from the compilation of Carmona *et al.* (2021). We used genus- or family-level means for seed size, SLA, and wood density values that were missing at the species level (15%, 28%, and 26%, respectively). We defined a species' seed productivity as (mass per seed) $\times$ (mean seeds per tree basal area) (Qiu *et al.*, 2022).

For species' climate, we extracted average temperature (in $^\circ$C) and moisture deficit (evapotranspiration minus precipitation, in mm) for each species based on all occurrences in the Global Biodiversity Information Facility (GBIF) through the R package `rgbif` (Chamberlain & Boettiger, 2017). The GBIF request is available from reference GBIF.org (2022). For species that are absent from GBIF, we extracted temperature and deficit from the MASTIF sites where those species were reported (162 species, 33%). Climate variables were obtained from CHELSA (Karger *et al.*, 2017).

Maturation and maximum size

To test the alternative hypotheses that the maturation diameter decreases ($\beta_d < 1$) or increases ($\beta_d > 1$) with maximum species size (Fig. 2b), we estimated parameters in Eq. (1) with the model

$$
\begin{aligned}
\log_{10}(d_{mat_s}) &= \log_{10}(\alpha) + \beta_d \times \log_{10}(d_{max_s}) + \cdots + \epsilon_s \\
\epsilon &\sim N(0, \sigma^2)
\end{aligned}
\tag{6}
$$

for species s, where the ellipsis includes climatic variables (moisture deficit and temperature) and their interactions with d_{max}. We tested alternative models including independence between maturation and maximum size (fitted α with β_d fixed at zero), proportionate increase (fitted α with $\beta_d = 1$), and changing relationship with size (both α and β_d estimated). Models were fitted with regression by using species average

14

estimates of d_{mat} as a response, and we included the inverse of the standard error of d_{mat} as weights. Model selection and fit were evaluated with AIC and root-mean-square error (RMSE). Regression dilution could cause underestimation of the strength between here d_{mat} and d_{max} when a predictor (i.e. d_{max}) contains errors (Frost & Thompson, 2000; Detto *et al.*, 2019). We thus ran additional analyses to test the robustness of our results to the regression dilution effect (see Supplementary material A.2). First, we corrected the parameter $\hat{\beta}_d$ from measurement error by using the R package `mecor` (Nab, 2021) (v1.0). Secondly, we tested if the relationship between d_{mat} and d_{max} varies depending on the origin of d_{max}.

Joint trait analysis

We evaluated the association between maturation size and other species' traits from the ability of d_{mat} to predict other trait values while allowing for climate and phylogeny effects (Fig. 2c). The marginal correlations that are commonly used for this purpose do not account for the many ways that traits can be related to one another. For instance, maturation size might be associated with maximum size because both tend to be high in warm climates, or in the phylogenetic groups that tend to occur in warm climates. To accommodate co-dependence between trait values we used Generalized Joint Attribute Modeling (GJAM) with traits as responses (Clark 2016). To account for phylogeny in the joint traits model, we diverged from traditional assumptions concerning residual covariance. Instead, we adopted a direct inference of the effects of phylogenetic groups. Traditional approaches of phylogenetic correction build on highly specific assumptions for the residual variance (random walk, or more complex models representing stabilizing selection such as the Ornstein–Uhlenbeck model). Our departure from these assumptions stems from the recognition that natural selection does not operate uniformly, neither within a given species pair nor across a broad spectrum of species. Our GJAM analysis explored phylogenetic contributions, with species groups treated as random effects and covariance that is unconstrained by assumptions on divergence rates (Qiu *et al.*, 2023). Explanatory variables included temperature, moisture deficit, and their interaction. Traits included wood density (g m^{-3}), specific leaf area (SLA) (mm^2 mg^{-1}), species seed productivity (kg m^{-2} basal area), seed size (g), maximum diameter (d_{max}) (cm), and maturation diameter (d_{mat}) (cm). All traits were log-transformed. We included a random phylogenetic group effect in the joint trait analysis (Qiu *et al.*, 2022; Bogdziewicz *et al.*, 2023; Qiu *et al.*, 2023). For species in speciose genera (more than 10 species), genus was used as the phylogenetic group. For species in less speciose genera but belonging to families with more than five species, family was used as the phylogenetic group. For the remaining species (<25% of the total), an 'other' category was used. To estimate the direct effect of traits (i.e. SLA, wood density, species seed productivity, seed size) and climatic variables on d_{mat}, we report conditional parameters from GJAM. Conditional parameters are estimated by extracting the parameters of the conditional distribution of traits conditioned on d_{mat}. Conditional parameters estimate the direct associations between traits while accounting for climate and phylogeny. Conditional parameters were obtained with the `gjam` R package (v2.6.2) (Supplementary Material, Section A.1).

Relation of d_{mat} along the phylogeny

We visualized how d_{rel} varies across species phylogeny by making a phylogenetic tree plot. We used the phylogeny from Zanne *et al.* (2014), and retrieved phylogenetic information for 400 out of the 486 studied species. Of the species missing from the phylogeny (i.e. 86 species), the relative proportion of missing phylogenetic information is about 13.2% for temperate species and about 19.4% for tropical species. We then tested for a phylogenetic signal in d_{rel} and d_{mat} using Pagel's λ (Pagel, 1999) (which test for a Brownian motion evolutionary signal), with values close to 0 indicating low phylogenetic signal and values close to 1 suggesting a phylogenetic correlation. We plotted the phylogenetic tree with `ggtree` R package (v3.8) (Yu *et al.*, 2017). We estimated the Pagel's λ by using the `phylosig` function from `phytools` (v1.5) (Revell, 2012).

Table 1: Coefficient estimates and fit to Eq. (6). The selected model with the lowest AIC (bold font at top) includes temperature (β_T) and the interaction between d_{max} and temperature (β_{dT}). The proportional cost model has β_d fixed at 1. The independence model has β_d fixed at 0. Additional models that include moisture deficit and temperature have higher AIC values (Table S4).

α	β_d	β_T	β_{dT}	σ	AIC	RMSE
3.71 [1.94, 7.07]	0.30 [0.15, 0.46]	-0.023 [-0.035, -0.011]	0.012 [0.0058, 0.019]	0.089	**-62**	10.2
1.08 [0.93, 1.25]	0.59 [0.55, 0.63]	-	-	0.090	-52	10.0
0.24 [0.23 , 0.26]	1	-	-	0.12	248	18.8
9.25 [8.69, 9.85]	0	-	-	0.15	447	15.4

Results

Maturation size is associated with maximum size, but not proportionately so (Fig. 3a). Large inter-specific variation in d_{mat} estimates had 95% quantiles that ranged from 4.0 to 51 cm, with relative maturation size ($d_{rel} = d_{mat}/d_{max}$) quantiles of (0.07, 0.65). Contrary to the baseline independence model ($\beta_d = 0$), trees did not start to reproduce at a constant size (dashed black line in Fig. 3a). If we force proportionality (fix β_d at 1), the estimate of $\hat{\alpha} = 0.24(0.23, 0.26)$ (line 3 of Table 1) is consistent with Loehle's (1988) range for hardwoods (1/5 to 1/4), but far outside his range for conifers (1/15 to 1/10). The 95% CI that is well below 0.5. This differs from the Visser *et al.* (2016)'s estimate of 1/2 for Barro Colorado Island (N = 60 species), Panama, and with Minor & Kobe (2019) La Selva, Costa Rica (N = 16 species). It is crucial to acknowledge that the aforementioned authors employed a distinct definition of d_{mat} and estimated larger d_{mat} (Fig. S3). Moreover, this proportional cost model ($\beta_d = 1$) fits poorly, with twice the RMSE and a higher AIC than the best-fitting model (Table 1).

Fitting both α and β_d (line 2 of Table 1) shows strong support for the diminishing risk model ($0 < \hat{\beta}_d < 1$). Allowing for environmental predictors further decreases the estimate to $\hat{\beta}_d = 0.30$ (0.15, 0.46). The exponent $0 < \beta_d < 1$ means that relative size at maturation (d_{rel}) decreases in large species (blue in Fig. 3a).

The best-fitting model (lowest AIC and RMSE) includes a negative effect of temperature (maturation at small size for species most common in cold climates) and a positive interaction between temperature T and d_{max} (Table 1). This positive interaction means that the relationship between maturation and maximum size
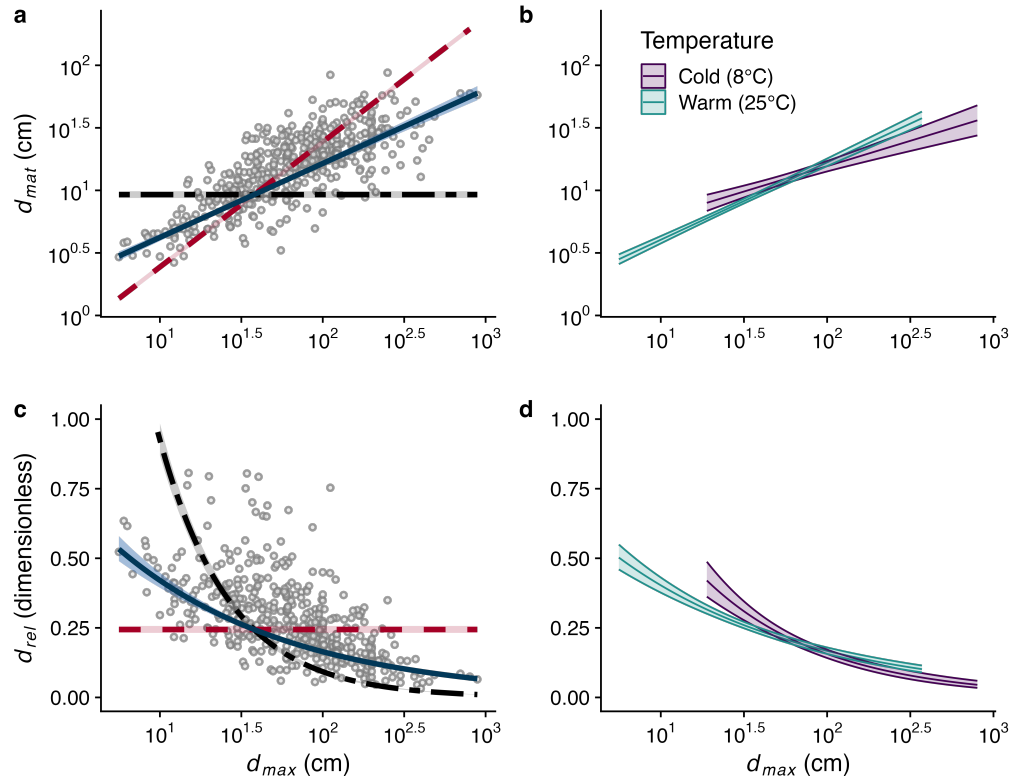
Figure 3: Tree maturation size (a, b), and relative size at maturation (c, d) for 486 species. Each dot represents one species. Alternative models are dashed lines, black for independence between maturation size and maximum size ($\beta_d = 0$), and red for the proportional cost model ($\beta_d = 1$). The best fitting model (blue with 95%CI) supports the diminishing risk model ($\beta_d < 1$, Table 1). Panels b and d are predictions from the fitted model with an interaction between continuous d_{max} and temperature (line 1 of Table 1). This model gives a continuous surface plot of maturation size as a function of maximum size and temperature (see Fig. S4). However, for clarity, we represent only the prediction at cold (8°C, purple) and warm temperatures (25°C, green) spanning observed diameter ranges.

tends to steepen for species in warm climates (Fig. 3b, d), approaching the proportionate risk model (Table 1); the rise in d_{mat} with d_{max} increases with temperature. However, the main plus interaction effect remains below 1 even in warm climates showing that the diminishing risk model is supported across this temperature range. The β_d remained below 1 even when we restricted the analysis to a single source of d_{max} (Table A1 and Figure A1, see Supplementary Section 2). After correcting for risks of regression dilution, the average value of β_d remained below 1, with corrected $\beta_d = 0.73$, however, the confidence interval is between 0.03 to 1.43 (Table A2, see Supplementary Section 2).
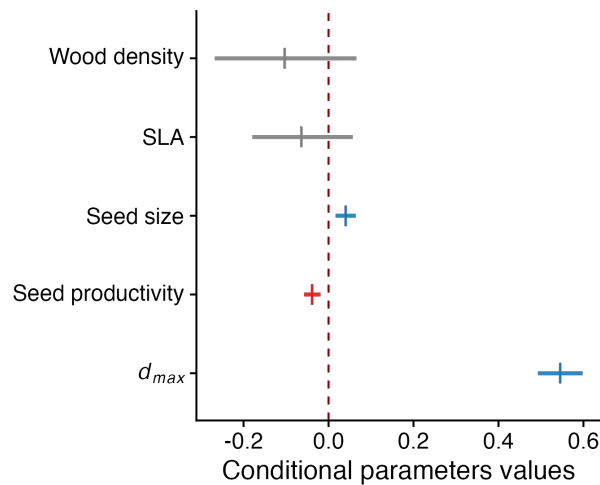

Figure 4: Conditional parameter estimates for the direct effect of traits on tree size at maturation diameter (d_{mat}) while accounting for trait covariance, climate, and phylogeny. Conditional parameters are evaluated on a standardized scale (predictors are centered and standardized) making trait effects on d_{mat} respective to their variation in the data set. Shown are posterior means and 95% credible intervals. Blue and red represent positive and negative associations where 95% of the posterior does not include zero. SLA = specific leaf area

The joint trait model incorporating random phylogenetic group and climate exhibits a root mean square prediction error 1.17 units smaller compared to the model that includes only climate. Conditional parameter estimates from the joint trait analysis show that d_{max} has a stronger effect on d_{mat} than other traits. There is a weak positive association with seed size, and a negative association with species fecundity (see Methods, Trait and climate data section) (Fig. 4). There are no meaningful associations with wood density or SLA. The joint trait analysis also confirms the absence of a direct climate effect on d_{mat} after accounting for d_{max} in the conditional trait analysis (see Table S5 for joint trait model and Table S6 for conditional parameters). Previous linear models showed that temperature was significant only in the interaction with d_{max} (Table S4). Joint trait analysis indicates that the temperature effect on maturation size in Fig. 2c could be due to the abundance of small species (small d_{max}) in warm climates (Figure S5). The trait relationships do not depend on the source of climatic data: i) GBIF species occurrence in Fig. 4 or ii) more narrowly, where they occur in the MASTIF data network (Fig. S6).

Both maturation (d_{mat}) and relative size (d_{rel}) show evidence of phylogenetic conservation ($\lambda_{mat} = 0.83$, $p < 0.0001$; $\lambda_{rel} = 0.51$, $p < 0.0001$, $n = 400$, Fig. S7a), yet with substantial variation within some groups.

18

The two-sample t-test for unequal variances shows differences between gymnosperms and angiosperms. Gymnosperms have high mean values for both d_{mat} and d_{max} and low mean values for d_{rel} (all $p < 0.0001$). Within gymnosperms, Pinales and Cupressaceae mature at large size, but large d_{max} gives them lower d_{rel} than most angiosperms (Fig. S8, S9). Most Pinaceae (*Picea*, *Pinus*) and Cupressaceae (*Thuja*, *Sequoia*), Fagaceae (*Quercus* and *Fagus*), and Juglandaceae have low d_{rel} (Fig. S10). Plant groups with both tree and shrub habits, such as Rosales, Magnoliales, Rubiaceae, and Fabaceae, have mixed d_{rel}. However, we did not find a significant effect of tree versus shrub habit on d_{rel}, possibly due to high variation in the data (Fig. S10). Shrubs may tend to have high d_{rel}, but higher d_{rel} is also observed in trees genera like *Magnolia* and *Poulsenia*.

Discussion

Our analysis suggests a diminishing risk model for the relationship between maturation and maximum size (i.e. d_{mat} and d_{max}). The novelty here comes from the low coupling we find. Indeed, the coefficient $\hat{\beta}_d = 0.30$ in Table 1 that we found is closer to zero (no relationship) than one. In contrast, the estimated exponent values fitted to vertebrates are greater than 1/2 (Prothero, 1993; Herculano-Houzel, 2019), twice the value of $\hat{\beta}_d$ we find for trees. Nevertheless, the comparison across groups is complex due to the uncertainty on maximum size (d_{max}), which could influence the value of the exponent $\hat{\beta}_d$, but this issue remained unexplored in other taxa. The biological difference of $\hat{\beta}_d$ may arise because trees differ from other species groups in the gains that come from allocation to growth, as the gain is due to the relative difference in height with other competitive individuals. In most tree species, individuals in the understory produce no seed at all, while dominant stature can yield multi-order-of-magnitude gains in fecundity over crowded neighbors (Clark *et al.*, 2004). In contrast, in vertebrates, improved parental condition and size can translate to incremental increases in clutch size or survival of well-provisioned offspring. Gestation times and physical limits on clutch size (e.g., one offspring) may allow only muted near-term benefits of reproductive delay.

In trees, large size comes with uncertainty that could weaken the potential benefit of delaying maturation. Wind exposure and risk of hydraulic failure both increase with size (Bennett *et al.*, 2015; Jackson *et al.*, 2021; Gardiner, 2021; Barrere *et al.*, 2023). The vanishing probability that a seed survives to large size, combined with the fact that fecundity can plateau and even decline late in life (Qiu *et al.*, 2021) means that the competitive advantages of extremely large size can rarely make up for lost benefits of early reproduction. At a stand scale, the risk of stand-replacing disturbances can increase with stand age and development (e.g., accumulated fuels increase fire risk), such that species that fail to reach minimum reproductive size before the next disturbance can be excluded from communities (Clark, 1991; McDowell *et al.*, 2020). The fact that maturation size increases with maximum size means that the two are not independent. But the cost is not proportionate (Fig. 3).

The fact that some correlation exists does not conflict with a disproportionate importance of near-term gains that can follow delayed maturation. Instead, it suggests that the benefits of large size probably do not come at the end of life. The capacity to reach a large size pays benefits throughout life, contributing with many other variables to current size and fecundity, not just as a tree approaches the maximum.

19

⁵⁰⁶ Both climate and species traits contribute to the relationships between maturation and maximum size. ⁵⁰⁷ The negative main effect of temperature and its positive interaction steepens the relationship with maximum ⁵⁰⁸ size in warm climates (Fig. 3), where growth and mortality rates are generally higher than in temperate forests ⁵⁰⁹ (Stephenson & Van Mantgem, 2005; Locosselli *et al.*, 2020). Abundant resources may offer a disproportionate ⁵¹⁰ advantage to early maturation (van Noordwijk & de Jong, 1986; Kozłowski, 1992; Wenk & Falster, 2015). Long ⁵¹¹ growing seasons in warm climates might have similar effects. However, intense competition on nutrient-rich ⁵¹² sites might also favor delayed reproduction as trees compete for canopy access. Theoretical studies (Falster ⁵¹³ *et al.*, 2017; Detto *et al.*, 2022) have shown that a trade-off between maximum size and maturation size can ⁵¹⁴ promote niche diversification and maintain species coexistence, and can be typically observed in tropical ⁵¹⁵ where there is a wide range of maximum sizes forests (Falster *et al.*, 2017).

⁵¹⁶ We did not find that high specific leaf area (SLA) is associated with maturation at small size (Visser ⁵¹⁷ *et al.*, 2016) or early age (Wenk *et al.*, 2018). The relationship reported in Wenk *et al.* (2018) includes leaf ⁵¹⁸ area from one year and one site, and the correlation estimated in that study does not appear to control for ⁵¹⁹ phylogeny. Similarly, lack of association with wood density in our study does not agree with suggestions that ⁵²⁰ shade-tolerant species with high wood density mature at small size (Thomas *et al.*, 2015). The inclusion of a ⁵²¹ wider range of plant species may reveal a different pattern of traits. For example, a comparison over a large ⁵²² number of perennial plant species such as herbs, graminoids, shrubs, and trees shows that traits that promote ⁵²³ longevity are associated with greater variability in seed production (Journé *et al.*, 2023). The fact that species ⁵²⁴ that produce large seeds also allocate more to reproductive effort (Qiu *et al.*, 2022) could contribute in a small ⁵²⁵ way to delayed maturation. The differences between our result and previous work may be due to the larger ⁵²⁶ species coverage, and to the control of the effect of climate and phylogeny in our joint analysis.

⁵²⁷ Results highlight the importance of large data sets and how they are modelled. This first compilation of ⁵²⁸ tree maturation size for hundreds of species on five continents shows strong support for a diminishing risk ⁵²⁹ model –trees that can get big can still mature at relatively small sizes. The result is a decline in the relative ⁵³⁰ size of maturation for large trees (Fig. 3d). The benefits of extensive data here parallel the shift from early ⁵³¹ theory that argued for a constant relative maturation size (d_{rel}) in fish (Charnov & Berrigan, 1990), followed ⁵³² by studies showing an exponent that is less than one (Froese & Binohlan, 2000; Tsikliras & Stergiou, 2014; ⁵³³ Thorson *et al.*, 2017). It is, however, important to acknowledge that our coverage of tree species diversity ⁵³⁴ is still patchy, with most data coming from Europe and North America and limited spatial coverage in Africa, ⁵³⁵ South America, Asia, and Oceania as data are concentrated in a few large plots in these areas (Daru & ⁵³⁶ Rodriguez, 2023).

⁵³⁷ New insight from this analysis comes first from extending observations beyond a small number of tropical ⁵³⁸ sites, few species, or limited sample size (Thomas, 1996; Wright *et al.*, 2005; Thomas, 2011; Visser *et al.*, ⁵³⁹ 2016; Minor & Kobe, 2019). The expanded coverage of species and sites permitted the incorporation of ⁵⁴⁰ climatic drivers into the analysis of d_{mat} in relation to d_{max}, which influenced the estimation of α and β_d. ⁵⁴¹ Secondly, this study also benefited from accommodating detection and temporal dependence to infer mat- ⁵⁴² uration. The estimation of d_{mat} was possible by combining diverse datasets, either based from direct crop ⁵⁴³ measurement and seed trap monitoring and by the use of MASTIF model which could estimate jointly a prob- ⁵⁴⁴ ability of maturation and individual fecundities. For instance, estimates of d_{mat} from Visser *et al.* (2016) are, ⁵⁴⁵ on average, approximately 1.8 times larger than our estimates for the species in common in the two studies

20

(Fig. S3). This discrepancy could be attributed to a different definition of size at maturation and methods of analysis, as our method also includes the number of seeds produced.

Due to the high juvenile mortality, the maturation sizes quantified here are expected to impact predictions from demographic vegetation models, including earth system models (ESMs) that include effects of maturation size. In one ESM study that considered the effects of maturation height, variation in a single value applied to all species did not have a large impact on simulated stand productivity (Raczka *et al.*, 2018). However, when differences in species maturation size are accounted for in models, the effect can be larger. Few individuals survive to large size and, thus, their ability to reproduce early can be important. The fact that species capable of large size tend to retain this capacity to reproduce while still small highlights the importance of understanding maturation size. Accurate estimation of maturation size (d_{mat}) is likewise important for assessing response to disturbance regimes, especially as the time to maturity begins to exceed the interval between disturbances. For instance, several species that compared pairs of species found that species with smaller size at maturation can have better post-disturbance dynamics than species with larger maturation size (Alfaro-Sánchez *et al.*, 2022; Andrus *et al.*, 2020). Our results provided the data to test such hypotheses at a much larger scale. This effect can even scale up at the ecosystem scale. In boreal habitats, exposure to more frequent disturbances that exceed the tree maturation time can completely change a tree community to a grass-dominated community without a return to a forest stand within centuries (Buma *et al.*, 2013).

Current ESMs suffer from limited information on allocation to reproduction (Wenk & Falster, 2015), including empirical data (Hanbury-Brown *et al.*, 2022b). Similarly, management actions intended to assure regeneration from seed also need to consider if the minimum harvest diameter is smaller than maturation size (Ouédraogo *et al.*, 2018). Maturation size may play an important role in the ability of species to respond to disturbance and climate change (McDowell *et al.*, 2020) when tree maturation can be reached faster under elevated CO_2 exposure (LaDeau & Clark, 2001). Considering the difference in maturation size between species may be crucial, although it can be more challenging to comprehend due to the impact of CO_2 on maturation size. Understanding how fecundity strategies differ between species and phylogenetic groups, such as lower relative size at maturation (d_{rel}) for gymnosperms than angiosperms, may open a new avenue to better understand species diversification and responses to disturbances (Bond, 1989; Verdu, 2002; Qiu *et al.*, 2022). Developing a model that represents the size at which a species begins to produce seeds could improve the representation of the regeneration of each functional type (Hanbury-Brown *et al.*, 2022a) and colonization rates (Snell, 2014) and improve our understanding of species coexistence. Our study contributes to the maturation sizes needed for each of these objectives.

References

Alfaro-Sánchez, R., Johnstone, J.F., Cumming, S.G., Day, N.J., Mack, M.C., Walker, X.J. *et al.* (2022). What Drives Reproductive Maturity and Efficiency in Serotinous Boreal Conifers? *Frontiers in Ecology and Evolution*, 10, 1–12.

Andrus, R.A., Harvey, B.J., Hoffman, A. & Veblen, T.T. (2020). Reproductive maturity and cone abundance vary with tree size and stand basal area for two widely distributed conifers. *Ecosphere*, 11.

Barrere, J., Reineking, B., Cordonnier, T., Kulha, N., Honkaniemi, J., Peltoniemi, M. *et al.* (2023). Functional traits and climate drive interspecific differences in disturbance-induced tree mortality. *Global Change Biology*, 29, 2836–2851.

Bennett, A.C., McDowell, N.G., Allen, C.D. & Anderson-Teixeira, K.J. (2015). Larger trees suffer most during drought in forests worldwide. *Nature Plants*, 1, 15139.

Bogdziewicz, M., Acuña, M.C.A., Andrus, R., Ascoli, D., Bergeron, Y., Brveiller, D. *et al.* (2023). Linking seed size and number to trait syndromes in trees. *Global Ecology and Biogeography*, 32, 683–694.

Bond, W.J. (1989). The tortoise and the hare: ecology of angiosperm dominance and gymnosperm persistence. *Biological Journal of the Linnean Society*, 36, 227–249.

Buma, B., Brown, C.D., Donato, D.C., Fontaine, J.B. & Johnstone, J.F. (2013). The impacts of changing disturbance regimes on serotinous plant populations and communities. *BioScience*, 63, 866–876.

Caignard, T., Kremer, A., Bouteiller, X.P., Parmentier, J., Louvet, J.M., Venner, S. *et al.* (2021). Countergradient variation of reproductive effort in a widely distributed temperate oak. *Functional Ecology*, 35, 1745–1755.

Caignard, T., Kremer, A., Firmat, C., Nicolas, M., Venner, S. & Delzon, S. (2017). Increasing Spring Temperatures Favor Oak Seed Production in Temperate Areas. *Scientific Reports*, 7, 1–8.

Carmona, C.P., Bueno, C.G., Toussaint, A., Träger, S., Díaz, S., Moora, M. *et al.* (2021). Fine-root traits in the global spectrum of plant form and function. *Nature*, 597, 683–687.

Chamberlain, S. & Boettiger, C. (2017). R python, and ruby clients for gbif species occurrence data. *PeerJ PrePrints*.

Charlesworth, B. (2000). Fisher, medawar, hamilton and the evolution of aging. *Genetics*, 156, 927–931.

Charnov, E.L. & Berrigan, D. (1990). Age of Maturity Versus the Adult Lifespan. *Evolutionary Ecology*, 4, 273–275.

Charnov, E.L. & Berrigan, D. (1991). Evolution of life history parameters in animals with indeterminate growth, particularly fish. *Evolutionary Ecology*, 5, 63–68.

22

608 Clark, J.S. (1991). Disturbance and tree life history on the shifting mosaic landscape. *Ecology*, 72, 1102–
609   1118.

610 Clark, J.S. (2016). Why species tell more about traits than traits about species: Predictive analysis. *Ecology*,
611   97, 1979–1993.

612 Clark, J.S., Andrus, R., Aubry-Kientz, M., Bergeron, Y., Bogdziewicz, M., Bragg, D.C. *et al.* (2021). Continent-
613   wide tree fecundity driven by indirect climate effects. *Nature Communications*, 12, 1–11.

614 Clark, J.S., Bell, D.M., Kwit, M.C. & Zhu, K. (2014). Competition-interaction landscapes for the joint response
615   of forests to climate change. *Global Change Biology*, 20, 1979–91.

616 Clark, J.S., LaDeau, S. & Ibanez, I. (2004). Fecundity of trees and the colonization–competition hypothesis.
617   *Ecological Monographs*, 74, 415–442.

618 Clark, J.S., Nuñez, C.L. & Tomasek, B. (2019). Foodwebs based on unreliable foundations: spatiotemporal
619   masting merged with consumer movement, storage, and diet. *Ecological Monographs*, 89, 1–24.

620 Clark, J.S., Silman, M., Kern, R., Macklin, E. & HilleRisLambers, J. (1999). Seed dispersal near and far:
621   Patterns across temperate and tropical forests. *Ecology*, 80, 1475–1494.

622 Daru, B.H. & Rodriguez, J. (2023). Mass production of unvouchered records fails to represent global biodi-
623   versity patterns. *Nature Ecology and Evolution*, 7, 816–831.

624 Davies, S.J. & Ashton, P.S. (1999). Phenology and fecundity in pioneer species of Euphorbiaceae. *American*
625   *Jornal of Botany*, 86, 1786–1795.

626 Detto, M., Levine, J.M. & Pacala, S.W. (2022). Maintenance of high diversity in mechanistic forest dynamics
627   models of competition for light. *Ecological Monographs*, 92.

628 Detto, M., Visser, M.D., Wright, S.J. & Pacala, S.W. (2019). Bias in the detection of negative density depen-
629   dence in plant communities. *Ecology Letters*, 22, 1923–1939.

630 Dietze, M.C. & Clark, J.S. (2008). Changing the gap dynamics paradigm: Vegetative regeneration control on
631   forest response to disturbance. *Ecological Monographs*, 78, 331–347.

632 Falster, D.S., Brännström, Å., Westoby, M. & Dieckmann, U. (2017). Multitrait successional forest dynamics
633   enable diverse competitive coexistence. *Proceedings of the National Academy of Sciences of the United*
634   *States of America*, 114, E2719–E2728.

635 Falster, D.S. & Westoby, M. (2003). Plant height and evolutionary games. *Trends in Ecology and Evolution*,
636   18, 337–343.

637 Feldpausch, T.R., Banin, L., Phillips, O.L., Baker, T.R., Lewis, S.L., Quesada, C.A. *et al.* (2011). Height-
638   diameter allometry of tropical forest trees. *Biogeosciences*, 8, 1081–1106.

Froese, R. & Binohlan, C. (2000). Empirical relationships to estimate asymptotic length, length at first maturity and length at maximum yield per recruit in fishes, with a simple method to evaluate length frequency data. *Journal of Fish Biology*, 56, 758–773.

Frost, C. & Thompson, S.G. (2000). Correcting for regression dilution bias: Comparison of methods for a single predictor variable. *Journal of the Royal Statistical Society. Series A: Statistics in Society*, 163, 173–189.

Gardiner, B. (2021). Wind damage to forests and trees: a review with an emphasis on planted and managed forests. *Journal of Forest Research*, 26, 248–266.

GBIF.org (2022). Occurrence download https://doi.org/10.15468/dl.wevh3v.

Hanbury-Brown, A.R., Powell, T.L., Muller-Landau, H.C., Wright, S.J. & Kueppers, L.M. (2022a). Simulating environmentally-sensitive tree recruitment in vegetation demographic models. *New Phytologist*, 235, 78–93.

Hanbury-Brown, A.R., Ward, R.E. & Kueppers, L.M. (2022b). Forest regeneration within Earth system models: current process representations and ways forward. *New Phytologist*, 235, 20–40.

Herculano-Houzel, S. (2019). Longevity and sexual maturity vary across species with number of cortical neurons, and humans are no exception. *Journal of Comparative Neurology*, 527, 1689–1705.

Jackson, T.D., Shenkin, A.F., Majalap, N., Bin Jami, J., Bin Sailim, A., Reynolds, G. *et al.* (2021). The mechanical stability of the world's tallest broadleaf trees. *Biotropica*, 53, 110–120.

Jensen, A.L. (1996). Beverton and Holt life history invariants result from optimal trade-off of reproduction and survival. 822, 820–822.

Journé, V., Andrus, R., Aravena, M.C., Ascoli, D., Berretti, R., Berveiller, D. *et al.* (2022). Globally, tree fecundity exceeds productivity gradients. *Ecology Letters*, 25, 1471–1482.

Journé, V., Hacket-Pain, A. & Bogdziewicz, M. (2023). Evolution of masting in plants is linked to investment in low tissue mortality. *Nature communications*, 14, 7998.

Karger, D.N., Conrad, O., Böhner, J., Kawohl, T., Kreft, H., Soria-Auza, R.W. *et al.* (2017). Climatologies at high resolution for the earth's land surface areas. *Scientific Data*, 4, 1–20.

Kattge, J., Díaz, S., Lavorel, S., Prentice, I.C., Leadley, P., Bönisch, G. *et al.* (2011). TRY - a global database of plant traits. *Global Change Biology*, 17, 2905–2935.

Koch, G.W., Stillet, S.C., Jennings, G.M. & Davis, S.D. (2004). The limits to tree height. *Nature*, 428, 851–854.

Kohler, P.K. & Huth, A. (2004). Simulating Growth Dynamics in a South-East Asian Rainforest Threatened By Recruitment Shortage and. *Climatic Change*, 67, 95–117.

670 Kohyama, T., Suzuki, E., Partomihardjo, T., Yamada, T. & Kubo, T. (2003). Tree species differentiation in
671   growth, recruitment and allometry in relation to maximum height in a Bornean mixed dipterocarp forest.
672   *Journal of Ecology*, 91, 797–806.

673 Kozłowski, J. (1992). Optimal allocation of resources to growth and reproduction: Implications for age and
674   size at maturity. *Trends in Ecology and Evolution*, 7, 15–19.

675 LaDeau, S.L. & Clark, J.S. (2001). Rising co2 levels and the fecundity of forest trees. *Science*, 292, 95–8.

676 Le Roncé, I., Gavinet, J., Ourcival, J.M., Mouillot, F., Chuine, I. & Limousin, J.M. (2021). Holm oak fecundity
677   does not acclimate to a drier world. *New Phytologist*, 231, 631–645.

678 Lines, E.R., Zavala, M.A., Purves, D.W. & Coomes, D.A. (2012). Predictable changes in aboveground allome-
679   try of trees along gradients of temperature, aridity and competition. *Global Ecology and Biogeography*, 21,
680   1017–1028.

681 Liu, H., Gleason, S.M., Hao, G., Hua, L., He, P., Goldstein, G. *et al.* (2019). Hydraulic traits are coordinated
682   with maximum plant height at the global scale. *Science Advances*, 5.

683 Locosselli, G.M., Brienen, R.J.W., Leite, M.d.S., Gloor, M., Krottenthaler, S., Oliveira, A.A.d. *et al.* (2020).
684   Global tree-ring analysis reveals rapid decrease in tropical tree longevity with temperature. *Proceedings of
685   the National Academy of Sciences*, 117, 33358–33364.

686 Loehle, C. (1988). Tree life history strategies: the role of defenses. *Canadian Journal of Forest Research*, 18,
687   209–222.

688 McDowell, N., Allen, C., Anderson-Teixeira, K., Aukema, B., Bond-Lamberty, B., Chini, L. *et al.* (2020). Perva-
689   sive shifts in forest dynamics in a changing world. *Science*, 368, eaaz9463.

690 Minor, D.M. & Kobe, R.K. (2019). Fruit production is influenced by tree size and size-asymmetric crowding in
691   a wet tropical forest. *Ecology and Evolution*, 9, 1458–1472.

692 Moles, A.T., Ackerly, D.D., Tweddle, J.C., Dickie, J.B., Smith, R., Leishman, M.R. *et al.* (2006). Global patterns
693   in seed size. *Global Ecology and Biogeography*, 16, 109–116.

694 Moles, A.T., Falster, D.S., Leishman, M.R. & Westoby, M. (2004). Small-seeded species produce more seeds
695   per square metre of canopy per year, but not per individual per lifetime. *Journal of Ecology*, 92, 384–396.

696 Nab, L. (2021). *mecor: Measurement Error Correction in Linear Models with a Continuous Outcome*. R
697   package version 1.0.0.

698 Niklas, K.J. (1994). *Plant Allometry. The Scaling of Form and Process.* Chicago.

699 van Noordwijk, A. & de Jong, G. (1986). Acquisition and Allocation of Resources: Their Influence on Variation
700   in Life History Tactics. *The American Naturalist*, 128, 137–142.

Ouédraogo, D.Y., Doucet, J.L., Daïnou, K., Baya, F., Biwolé, A.B., Bourland, N. *et al.* (2018). The size at reproduction of canopy tree species in central Africa. *Biotropica*, 50, 465–476.

Pagel, M. (1999). Inferring the historical patterns of biological evolution. *Nature*, 401, 877–884.

Prothero, J. (1993). Adult life span as a function of age at maturity. *Experimental Gerontology*, 28, 529–536.

Qiu, T., Andrus, R., Aravena, M.C., Ascoli, D., Bergeron, Y., Berretti, R. *et al.* (2022). Limits to reproduction and seed size-number trade-offs that shape forest dominance and future recovery. *Nature Communications*, 13.

Qiu, T., Aravena, M.C., Andrus, R., Ascoli, D., Bergeron, Y., Berretti, R. *et al.* (2021). Is there tree senescence? The fecundity evidence. *Proceedings of the National Academy of Sciences of the United States of America*, 118, 1–10.

Qiu, T., Aravena, M.C., Ascoli, D., Bergeron, Y., Bogdziewicz, M., Boivin, T. *et al.* (2023). Masting is uncommon in trees that depend on mutualist dispersers in the context of global climate and fertility gradients. *Nature Plants*, 9, 1044–1056.

R Core Team (2023). *R: A Language and Environment for Statistical Computing*. R Foundation for Statistical Computing, Vienna, Austria.

Raczka, B., Dietze, M.C., Serbin, S.P. & Davis, K.J. (2018). What limits predictive certainty of long-term carbon uptake? *Journal of Geophysical Research: Biogeosciences*, 123, 3570–3588.

Revell, L.J. (2012). phytools: An R package for phylogenetic comparative biology (and other things). *Methods in Ecology and Evolution*, 3, 217–223.

Seyednasrollah, B. & Clark, J.S. (2020). Where Resource-Acquisitive Species Are Located: The Role of Habitat Heterogeneity. *Geophysical Research Letters*, 47, 1–12.

Sharma, S., Andrus, R., Bergeron, Y., Bogdziewicz, M., Bragg, D.C., Brockway, D. *et al.* (2022). North American tree migration paced by climate in the West, lagging in the East. *Proceedings of the National Academy of Sciences of the United States of America*, 119.

Snell, R.S. (2014). Simulating long-distance seed dispersal in a dynamic vegetation model. *Global Ecology and Biogeography*, 23, 89–98.

Stearns, S.C. (1989). Trade-Offs in Life-History Evolution. *Functional Ecology*, 3, 259–268.

Stephenson, N.L. & Van Mantgem, P.J. (2005). Forest turnover rates follow global and regional patterns of productivity. *Ecology Letters*, 8, 524–531.

Thomas, S.C. (1996). Relative size at onset of maturity in rain forest trees: a comparative analysis of 37 Malaysian species. *Oikos*, 76, 1450154.

732 Thomas, S.C. (2011). Age-Related Changes in Tree Growth and Functional Biology: The Role of Reproduc-
733   tion. In: *Size- and Age-Related Changes in Tree Structure and Function* (eds. Meinzer, F.C., Lachenbruch,
734   B. & Dawson, T.E.). Springer Netherlands, Dordrecht, vol. 4, pp. 33–64.

735 Thomas, S.C., Martin, A.R. & Mycroft, E.E. (2015). Tropical trees in a wind-exposed island ecosystem:
736   Height-diameter allometry and size at onset of maturity. *Journal of Ecology*, 103, 594–605.

737 Thorson, J.T., Munch, S.B., Cope, J.M. & Gao, J. (2017). Predicting life history parameters for all fishes
738   worldwide. *Ecological Applications*, 27, 2262–2276.

739 Tsikliras, A.C. & Stergiou, K.I. (2014). Size at maturity of Mediterranean marine fishes. *Reviews in Fish
740   Biology and Fisheries*, 24, 219–268.

741 Verdu, M. (2002). Age at maturity and diversification in woody angiosperms´. *Evolution*, 56, 1352–1361.

742 Visser, M.D., Bruijning, M., Wright, S.J., Muller-Landau, H.C., Jongejans, E., Comita, L.S. *et al.* (2016).
743   Functional traits as predictors of vital rates across the life cycle of tropical trees. *Functional Ecology*, 30,
744   168–180.

745 Wallentin, G., Tappeiner, U., Strobl, J. & Tasser, E. (2008). Understanding alpine tree line dynamics: An
746   individual-based model. *Ecological Modelling*, 218, 235–246.

747 Wenk, E.H., Abramowicz, K., Westoby, M. & Falster, D.S. (2018). Investment in reproduction for 14 iteroparous
748   perennials is large and associated with other life-history and functional traits. *Journal of Ecology*, 106,
749   1338–1348.

750 Wenk, E.H. & Falster, D.S. (2015). Quantifying and understanding reproductive allocation schedules in plants.
751   *Ecology and Evolution*, 5, 5521–5538.

752 Westoby, M., Falster, D.S., Moles, A.T., Vesk, P.A. & Wright, I.J. (2002). Plant ecological strategies: Some
753   leading dimensions of variation between species. *Annual Review of Ecology and Systematics*, 33, 125–
754   159.

755 Wright, S.J., Jaramillo, M.A., Pavon, J., Condit, R., Hubbell, S.P. & Foster, R.B. (2005). Reproductive size
756   thresholds in tropical trees: Variation among individuals, species and forests. *Journal of Tropical Ecology*,
757   21, 307–315.

758 Yang, X., Angert, A.L., Zuidema, P.A., He, F., Huang, S., Li, S. *et al.* (2022). The role of demographic
759   compensation in stabilising marginal tree populations in North America. *Ecology Letters*, 25, 1676–1689.

760 Yu, G., Smith, D.K., Zhu, H., Guan, Y. & Lam, T.T.Y. (2017). Ggtree: an R Package for Visualization and
761   Annotation of Phylogenetic Trees With Their Covariates and Other Associated Data. *Methods in Ecology
762   and Evolution*, 8, 28–36.

763 Zanne, A.E., Tank, D.C., Cornwell, W.K., Eastman, J.M., Smith, S.A., FitzJohn, R.G. *et al.* (2014). Three keys
764   to the radiation of angiosperms into freezing environments. *Nature*, 506, 89–92.

Acknowledgements

Competing interests

The authors declare no competing interests

Supplementary Materials

Section A1 - A2

Table S1 – S6

Fig S1 - S9

Supplementary material

A.1   Conditional parameters

One way to evaluate relationships between traits is to ask how well a trait like d_{mat} predicts other traits, while
controlling for effects of climate and phylogeny. We start with the joint distribution of M traits for each species
$s = 1, \ldots, S$ fitted with GJAM (Methods). All traits were log-transformed. The joint distribution is

$$[\mathbf{T}_s | P, X] = MVN_M(\mathbf{T}_s | \mathbf{B}'\mathbf{x}_s + \mathbf{g}[s], \Sigma)$$
$$\mathbf{g} \sim MVN(\mathbf{0}, \Omega) \tag{A1}$$

where MVN is the multivariate normal distribution, $\mathbf{g}[s]$ is a random vector for the phylogenetic group to which
s belongs, and Ω is the $M \times M$ covariance between traits taken over phylogenetic groups (Clark *et al.*, 2016).
With this fitted model, we consider the effects of d_{mat} on all other traits, organized in the vector $\mathbf{T} = [\mathbf{u}, \mathbf{d}]$,
where $\mathbf{d}$ is the length-S vector of maturation sizes, and $\mathbf{u}$ is a $S \times M - 1$ matrix holding all traits in $\mathbf{T}$ other
than d_{mat}.

We partition the coefficients in $\mathbf{B}$ and trait covariance Σ as

$$\mathbf{B} = \begin{bmatrix} \mathbf{B}_u \\ \mathbf{B}_d \end{bmatrix}, \Sigma = \begin{bmatrix} \Sigma_{u,u} & \Sigma_{u,d} \\ \Sigma_{d,u} & \Sigma_{d,d} \end{bmatrix} \tag{A2}$$

For M traits and Q climate predictors in $\mathbf{x}_s$, $\mathbf{B}_u$ is the $Q \times M - 1$ matrix of climate effects on traits other
than d_{mat}, $\mathbf{B}_d$ is the $Q \times 1$ vector of climate effects on d_{mat}, with similar partition of Σ. We then write the
conditional distribution of responses in $\mathbf{u}$ as

$$\mathbf{u}_s | d_{mat,s} \sim MVN(\mathbf{A}d_{mat,s} + \mathbf{C}\mathbf{x}_s + \mathbf{g}[s], \mathbf{P})$$
$$\mathbf{A} = \Sigma_{u,d}\Sigma_{d,d}^{-1}$$
$$\mathbf{C} = \mathbf{B}'_u - \mathbf{A}\mathbf{B}'_d \tag{A3}$$
$$\mathbf{P} = \Sigma_{u,u} - \mathbf{A}\Sigma_{d,u}$$

$\mathbf{A}$ is the vector of effects of d_{mat} on each response in $\mathbf{u}$, $\mathbf{C}$ holds the effects of $\mathbf{x}$, and $\mathbf{P}$ is the conditional
residual covariance. Other applications can be found in Qiu *et al.* (2021); Bogdziewicz *et al.* (2023). We report
in Fig. 4 the estimates from $\mathbf{A}$.

A.2 Impact of error on estimates of maximum size (d_{max})

A.2.1 Robustness of the model relating maturation size to maximum size to data sources

In this additional analysis, we aimed to test the relationship between maturation size (d_{mat}) and maximum size (d_{max}) using different data sources for d_{max}. The estimates d_{max} used in the main analysis are based on online open sources and are on average higher than other sources of d_{max} (Figure S2) which could underestimate the parameter β_d. The analysis was restricted to the most abundant data source of d_{max}. We conducted separate regression analyses using d_{max} estimates from unpublished data (J. Wright, N = 233 species), National Forest Inventories (N = 158 species), and MASTIF inventories (N = 346 species) based on the model from Equation (6). In the three different models (i.e. one model per data source of d_{max}), we used the inverse of the standard error of d_{mat} as weights in the models. We then extracted coefficient estimates for all three models. Results are reported in Table A1 and visualized in Figure A1.

Table A1: Coefficient estimates from the model Eq. (6) according to the origin of d_{max}. Data sources of d_{max} are National Forest Inventories (NFI), MASTIF inventories, and unpublished field tropical measurements.

Origin of d_{max}	α	β_d	σ
NFI	1.40 [0.89, 2.20]	0.56 [0.45, 0.68]	0.089
MASTIF	1.30 [1.10, 1.60]	0.64 [0.58, 0.70]	0.078
Unpublished	0.88 [0.73, 1.10]	0.65 [0.60, 0.70]	0.090
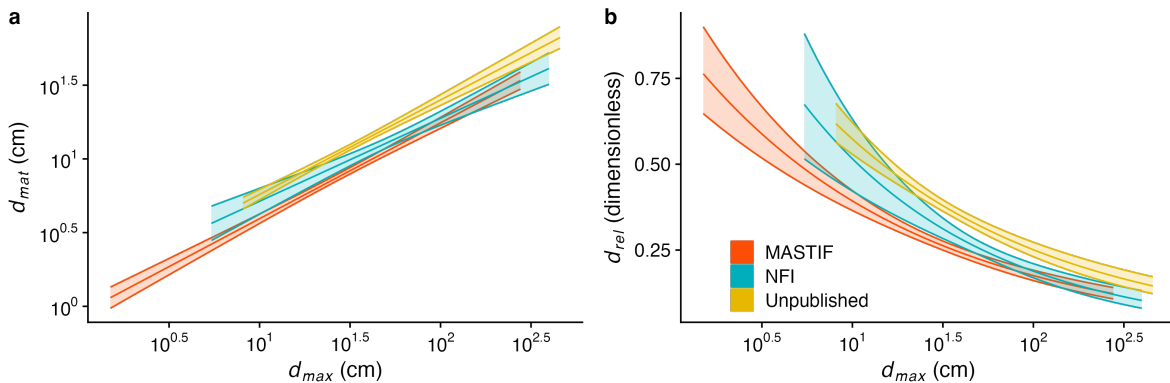
Figure A1: Tree maturation size and relative size at maturation relationship to maximum size according to the origin of maximum size observations. The orange line represents predictions from the regression between d_{mat} and d_{max} based on unpublished data (obtained from J. Wright field observation, N = 233 species). In blue, the prediction from the regression between d_{mat} and d_{max} comes only from National Forest Inventories estimates (N = 158 species). In yellow, the prediction from the regression between d_{mat} and d_{max} comes only from MASTIF inventories (N = 346 species).

A.2.2 Correction of maximum size error measurement

Measurement error in a covariate is common and often ignored which could have implications in the estimation of the relationship between a response and a covariate (Nab *et al.*, 2021). Indeed, the true value of a covariate, here of d_{max}, is not available, and using a log-log model exposed to regression dilution could flatten the slope (β_d) (Detto *et al.*, 2019). To correct for measurement error we benefit here from the R package `mecor` (Nab, 2021) by using additional observation of our variable d_{max}. We specified here the error-prone measurement of d_{max}, coming from the highest estimates of d_{max}. We then used here four different additional observations of d_{max}, where this covariate can be obtained from Online Open-access resources, National Forest Inventories, Unpublished data, and MASTIF inventories. We ran the analysis on a simple model from Equation (6), that would include only d_{max}, or both d_{max} and temperature as covariates. The function does not allow to take into account weights in the analysis. To make a fair comparison, we reported here both coefficients, uncorrected and corrected (Table A2).

Table A2: Coefficient estimates uncorrected and corrected from measurement errors fitted to Eq. (6). Values are reported with a mean estimate and 95% CI.

Model	Coefficient Parameter	Uncorrected value	Corrected value
$d_{max}; T$	α	1.404 [1.092, 1.804]	0.826 [0.022, 31.637]
	β_d	0.58 [0.53, 0.62]	0.732 [-0.049, 1.51]
	β_T	-0.0005 [-0.0029, 0.0019]	-0.0003 [-0.012, 0.011]
d_{max}	α	1.357 [1.132, 1.627]	0.810 [0.048, 13.555]
	β_d	0.582 [0.539, 0.625]	0.733 [0.031, 1.434]

31

Supplementary Tables and Figures

Table S1: Numbers of species, plots, tree-year observations coming from crop count and seeds traps, and individual species tree year observations according to region. Additional details about MASTIF network are provided in Supplementary Files 1 and 2, and in Table S2.

Region	Nb. of plots	Nb. of species	Crop count x year	Seed-trap x year	Nb. Ind/Year
Africa	2	19	416	9,705	12
Asia	4	59	0	1,589,946	1,475
Eastern North America	155	92	20,983	1,389,998	142
Western North America	280	29	83,042	715,132	576
Europe	156	21	30,763	158,991	28
South America	7	267	2,280	7,050,620	863

Table S2: MASTIF plots listed by WWF eco-regions, with principal investigator list and references. The column ST/CC indicates seed traps (ST) and crop counts (CC) sites.

Eco-region	Plot	PI(s)	lon	lat	ST/CC	Citation
A/W Turkey sclerophyllous/mixed						
	PNPG	E. Daskalakou	24	38	CC	Daskalakou *et al.* (2019)
Alps conifer/mixed forests						
	ROTH	G. Gratzer	15	48	ST	
	BELLE	G. Kunstler; B. Courbaud	6	45	ST CC	
	RNNPT	L. Dormon	7	45	CC	Dormont *et al.* (2006)
	PNPP	D. Ascoli; R. Motta; R. Berretta; G. Vacchiano	12	46	ST	Hacket-Pain *et al.* (2019)
Appalachian-Blue Ridge forests						
	BCEF	C. Greenberg	-83	35	CC	Rose *et al.* (2012)
	CWT	J. S. Clark	-83	35	ST CC	Clark *et al.* (2004)
	EPENN	M. Steele	-76	41	CC	
	GRAN	C. Greenberg	-82	36	CC	Rose *et al.* (2012)
	GRSM	J. S. Clark	-83	36	ST	
	MARS	J. S. Clark; S. Pearson	-83	36	ST CC	Clark *et al.* (2014)
	MLBS	J. S. Clark	-81	37	ST CC	
	PISG	C. Greenberg	-83	35	CC	Rose *et al.* (2012)
	SCBI	B. McShea	-78	39	ST	Bourg *et al.* (2013)
Appalachian mixed mesophytic forests						
Arizona Mountains forests						
	MOPA	M. Redmond	-106	33	CC	Redmond *et al.* (2012)
	REMO	A. Whipple; C. Gering; T. Whitham	-112	36	CC	Whipple *et al.* (2019)
	SICI	A. Wion; M. Redmond	-108	33	CC	
	WHIT	A. Wion; M. Redmond	-109	33	CC	
	WINO	A. Whipple; C. Gering; T. Whitham	-111	35	CC	Whipple *et al.* (2019)

Eco-region	Plot	PI(s)	lon	lat	ST/CC	Citation
Atlantic coastal pine barrens						
	BARBEAU	N. Delpierre; D. Berveiller	3	48	ST	
Atlantic mixed forests						
Balkan mixed forests						
Baltic mixed forests						
British Columbia mainland coastal forests						
	GLCR1	J. Franklin	-122	49	CC	
	GLCR2	J. Franklin	-122	49	CC	
	HEME	J. Franklin	-122	49	CC	
	STPA	J. Franklin	-121	47	CC	
California Central Valley grasslands						
California interior chaparral/woodlands						
California montane chaparral/woodlands						
	HNHR	J. Knops; W. Koenig	-122	36	CC	Knops & Koenig (2012)
Carpathian montane forests						
	BGNP	M. Zywiec; L. Piechnik; B. Seget; M. Ledwon	20	50	CC	
Cascade Mountains leeward forests						
	TUCR	J. Franklin	-121	48	CC	
Celtic broadleaf forests						
	BENWE	A. Hacket-Pain	-2	55	CC	Bogdziewicz *et al.* (2020)
	CONGL	A. Hacket-Pain	-2	53	CC	Bogdziewicz *et al.* (2020)
	GILLF	A. Hacket-Pain	-2	54	CC	Bogdziewicz *et al.* (2020)
	HIMLE	A. Hacket-Pain	-2	53	CC	Bogdziewicz *et al.* (2020)
	KEELE	A. Hacket-Pain	-2	53	CC	Bogdziewicz *et al.* (2020)
	KILLE	A. Hacket-Pain	-3	51	CC	Bogdziewicz *et al.* (2020)
	RIPON	A. Hacket-Pain	-1	54	CC	Bogdziewicz *et al.* (2020)
	SPENN	A. Hacket-Pain	-2	55	CC	Bogdziewicz *et al.* (2020)

Eco-region	Plot	PI(s)	lon	lat	ST/CC	Citation
	WOODB	A. Hacket-Pain	-3	51	CC	Bogdziewicz *et al.* (2020)
Central Canadian Shield forests						
	COCH	Y. Bergeron; Y. Messaoud	-81	49	CC	Messaoud *et al.* (2007)
	LDUPT	Y. Bergeron; Y. Messaoud	-79	48	CC	Messaoud *et al.* (2007)
	MASK	Y. Bergeron; Y. Messaoud	-79	50	CC	Messaoud *et al.* (2007)
Central European mixed forests						
Central forest-grasslands transition						
	UKFS	J. S. Clark	-95	39	ST CC	
	WUSL	J. Myers	-91	39	ST	
Central Pacific coastal forests						
	MAPK	J. Franklin	-124	45	CC	
Central Ranges xeric scrub						
	LS	B. Wright	132	-24	CC	Wright & Zuur (2014)
Central tall grasslands						
Central/S Cascades forests						
	BAMT	J. Franklin	-122	46	ST	
	BERK	J. Franklin	-122	43	CC	
	BLLK	J. Franklin	-122	46	CC	
	DECU	J. Franklin	-122	45	CC	
	IRMT	J. Franklin	-122	44	CC	
	MOLK	J. Franklin	-122	46	CC	
	MORA	J. HilleRisLambers	-122	47	ST	
	PEPR	J. Franklin	-122	46	CC	
	SAMT	J. Franklin	-122	44	CC	Redmond *et al.* (2012)
	SAPA	J. Franklin	-122	45	CC	
	SIRK	J. Franklin	-122	46	CC	
	SLBE	J. Franklin	-122	46	CC	

Eco-region	Plot	PI(s)	lon	lat	ST/CC	Citation
	STMT	J. Franklin	-122	46	CC	
	TIRD	J. Franklin	-122	46	CC	
	WIMT1	J. Franklin	-122	44	CC	
	WIMT2	J. Franklin	-122	44	CC	
	WISP	J. Franklin	-122	43	CC	
	WREF	J. S. Clark; J. HilleRisLambers	-122	46	ST CC	
Chihuahuan desert						
	FOBA	M. Redmond	-108	33	CC	Redmond *et al.* (2012)
Colorado Plateau shrublands						
	ALBU	A. Wion; M. Redmond	-106	35	CC	Wion *et al.* (2020)
	CEBO	A. Wion; M. Redmond	-106	36	CC	Rodman *et al.* (2020)
	DOLO	A. Wion; M. Redmond	-109	38	CC	Rodman *et al.* (2020)
	GLPA	A. Wion; M. Redmond	-109	39	CC	Rodman *et al.* (2020)
	HOND	A. Wion; M. Redmond; K. Rodman	-106	37	CC	
	HOTC	A. Wion; M. Redmond; K. Rodman	-108	39	CC	Rodman *et al.* (2020)
	LASA	A. Wion; M. Redmond	-109	39	CC	Rodman *et al.* (2020)
	MAGD	A. Wion; M. Redmond	-107	34	CC	Rodman *et al.* (2020)
	MONT	A. Wion; M. Redmond	-108	38	CC	Rodman *et al.* (2020)
	NATU	A. Wion; M. Redmond	-109	38	CC	Rodman *et al.* (2020)
	SEV	R. Zlotin; D. Macias	-107	34	CC	Parmenter *et al.* (2018)
	SUCR	A. Whipple; C. Gering; T. Whitham	-111	36	CC	Whipple *et al.* (2019)
Colorado Rockies forests						
	BOCA	I. Pearse	-105	40	CC	
	CANJ	A. Wion; M. Redmond	-106	36	CC	Rodman *et al.* (2020)
	HAYM	A. Wion; M. Redmond	-105	39	CC	
	LAK	K. Rodman	-106	36	CC	Rodman *et al.* (2020)
	LV	M. Redmond	-105	36	CC	Redmond *et al.* (2012)

Eco-region	Plot	PI(s)	lon	lat	ST/CC	Citation
	MG	K. Rodman	-106	36	CC	Rodman *et al.* (2020)
	MON	K. Rodman	-106	36	CC	Rodman *et al.* (2020)
	MR	K. Rodman	-106	36	CC	Rodman *et al.* (2020)
	MVG	K. Rodman	-106	36	CC	Rodman *et al.* (2020)
	NIWO	J. S. Clark	-106	40	ST CC	
	PC	K. Rodman	-106	36	CC	Rodman *et al.* (2020)
	PECO	M. Redmond	-106	36	CC	Redmond *et al.* (2012)
	POND	A. Wion; M. Redmond	-107	36	CC	Wion *et al.* (2020)
	RATN	M. Redmond	-104	37	CC	Redmond *et al.* (2012)
	SAFE	A. Wion; M. Redmond	-106	36	CC	Rodman *et al.* (2020)
	WACA	A. Wion; M. Redmond	-105	39	CC	
	WEMO	A. Wion; M. Redmond	-105	38	CC	
Cross-Sanaga-Bioko coastal forests						
	KNP	J. Norghauer	9	5	CC	Norghauer & Newbery (2015)
Dinaric Mountains mixed forests						
E Cascades forests						
E forest-boreal transition						
	LMONT	Y. Bergeron; Y. Messaoud	-79	48	CC	Messaoud *et al.* (2007)
E Great Lakes lowland forests						
English Lowlands beech forests						
	BEECH	A. Hacket-Pain	0	52	CC	Bogdziewicz *et al.* (2020)
	BUCKH	A. Hacket-Pain	-2	52	CC	Bogdziewicz *et al.* (2020)
	FISHH	A. Hacket-Pain	-2	52	CC	Bogdziewicz *et al.* (2020)
	NETTL	A. Hacket-Pain	-1	52	CC	Bogdziewicz *et al.* (2020)
	PAINS	A. Hacket-Pain	-2	52	CC	Bogdziewicz *et al.* (2020)
	PATCH	A. Hacket-Pain	-0	51	CC	Bogdziewicz *et al.* (2020)
	STP	M. Fenner M. Hanley	-1	51	CC	Hanley *et al.* (2018)

Eco-region	Plot	PI(s)	lon	lat	ST/CC	Citation
Great Basin shrub steppe						
	DSP	M. Redmond	-119	39	CC	
Iberian sclerophyllous/semi-deciduous						
	CARB	C. Perez-Izquierdo	-6	40	CC	
	HUEC	R. Bonal	-4	40	CC	
	SIOE	R. Calama	-4	40	CC	
	VALT	J. Espelta	-4	41	CC	
Illyrian deciduous forests						
Interior Alaska-Yukon lowland taiga						
	EAPL	J. Johnstone	-137	66	CC	Viglas *et al.* (2013)
	BONA	J. Johnstone	-148	65	ST	
	FAIR	J. Johnstone	-148	65	CC	Viglas *et al.* (2013)
	LAGE	J. Johnstone	-145	64	CC	Viglas *et al.* (2013)
	LELA	J. Johnstone	-138	64	CC	Viglas *et al.* (2013)
	SMR	J. Johnstone	-141	64	CC	Viglas *et al.* (2013)
Interior Yukon-Alaska alpine tundra						
	CHIC	J. Johnstone	-143	63	CC	Viglas *et al.* (2013)
Isthmian-Atlantic moist forests						
	BCI	S.J. Wright	-80	9	ST	
Italian sclerophyllous/semi-deciduous						
Klamath-Siskiyou forests						
	ASRN	J. Franklin	-123	42	CC	
	MEOV	J. Franklin	-123	42	CC	
Mid Atlantic coastal forests						
	BLSF	D. Brockway	-79	35	CC	Chen *et al.* (2018)
	CALL	J. S. Clark	-79	35	ST CC	
	CROA	S. Cohen	-77	35	CC	

Eco-region	Plot	PI(s)	lon	lat	ST/CC	Citation
	GRSW	J. S. Clark	-78	34	ST	
	SASF	D. Brockway	-81	34	CC	Chen *et al.* (2018)
Mississippi lowland forests						
	CHICK	J. Straub; T. Leininger	-90	36	CC	Straub *et al.* (2016)
	DELTA	J. Straub; T. Leininger	-91	33	CC	Straub *et al.* (2016)
	MINGO	J. Straub; T. Leininger	-90	37	CC	Straub *et al.* (2016)
	TENAS	J. Straub; T. Leininger	-91	32	CC	Straub *et al.* (2016)
	WHITE	J. Straub; T. Leininger	-91	34	CC	Straub *et al.* (2016)
Montana Valley/Foothill grasslands						
N California coastal forests						
	UCSC	G. Gilbert; Kai Zhu	-122	37	ST	
N Central Rockies forests						
	WBP	E. McIntire	-114	48	CC	
N short grasslands						
NE coastal forests						
NE Spain/S France Mediterranean						
	ISS	H. Davi	6	44	CC	Davi *et al.* (2016)
	PCMEJEAN	T. Curt	3	44	CC	Debain *et al.* (2003)
	PUECHEXP1	J. Limousin; J. Ourcival	4	44	ST	
	RBI	T. Boivin	5	44	CC	Doublet *et al.* (2019)
	RBLL	H. Davi	6	44	CC	Davi *et al.* (2016)
	VALLI	F. Lefevre; F. Courbet	5	44	CC	
	VEN	H. Davi	5	44	CC	Davi *et al.* (2016)
	VENT	H. Davi	5	44	CC	Davi *et al.* (2016)
	VES	H. Davi	7	44	CC	Davi *et al.* (2016)
New England-Acadian forests						
	ASWP	C. Moore; J. S. Clark	-69	45	ST CC	

Eco-region	Plot	PI(s)	lon	lat	ST/CC	Citation
	BART	I. Fer; M. Dietze	-71	44	ST	
	COMPT	W. Schlesinger	-67	45	CC	
	HARV	J. S. Clark	-72	42	ST CC	
	HBEF	T. Fahey; N. Cleavitt	-72	44	ST	Cleavitt & Fahey (2017)
Nihonkai montane deciduous forests						
	KANU	K. Hoshizaki	141	39	ST	
	JNP	Q. Han; D. Kabeya; K. Noguchi	139	37	ST	Han *et al.* (2014)
NW Congolian lowland forests						
	CONGO	J. Poulson; C. Nunez	16	2	ST	
Pannonian mixed forests						
Peruvian Yungas						
	ABERG	M. Silman; W. Farfan	-72	-13	ST	
Piney Woods forests						
	KINF	D. Brockway	-92	31	CC	Chen *et al.* (2018)
Pontic steppe						
Puerto Rican dry forests						
	GUA	M. Uriarte	-67	18	ST	Uriarte *et al.* (2012)
Puerto Rican moist forests						
	LUQ	M. Uriarte	-66	18	ST	Uriarte *et al.* (2012)
Puget lowland forests						
Pyrenees conifer/mixed forests						
	PNVO	J. Camarero	-1	43	ST	de Andrés *et al.* (2014)
	PNP	S. Delzon; T. Caignard	-0	43	CC	Caignard *et al.* (2017)
Rodope montane mixed forests						
S Central Rockies forests						
	YELL	J. S. Clark	-110	45	ST CC	
S Great Lakes forests						

Eco-region	Plot	PI(s)	lon	lat	ST/CC	Citation
	ANNA	I. Ibanez	-84	42	ST	Redmond *et al.* (2012)
SE conifer forests						
	APNF	D. Brockway	-85	30	CC	Chen *et al.* (2018)
	BRSF	D. Brockway	-87	31	CC	Chen *et al.* (2018)
	DSNY	J. S. Clark	-81	28	ST CC	
	EAFB	D. Brockway	-87	30	CC	Chen *et al.* (2018)
	EEF	D. Brockway	-87	31	CC	Chen *et al.* (2018)
	JERC	D. Brockway	-84	31	CC	Chen *et al.* (2018)
	OSBS	J. S. Clark	-82	30	ST CC	
	STCB	D. Brockway	-85	31	CC	Chen *et al.* (2018)
	TTRS	D. Brockway	-86	31	CC	Chen *et al.* (2018)
SE mixed forests						
	DUKE	J. S. Clark	-79	36	ST CC	Berdanier & Clark (2016)
	FBMB	D. Brockway	-85	32	CC	Chen *et al.* (2018)
	SERC	J. S. Clark	-77	39	ST CC	van Mantgem *et al.* (2006)
	TALL	J. S. Clark	-87	33	ST CC	
Sierra Nevada forests						
	SEQU	A. Das; N. Stephenson	-119	37	ST	van Mantgem *et al.* (2006)
	SOAP	J. S. Clark	-119	37	ST CC	
	YOSE	A. Das; N. Stephenson	-120	38	ST	van Mantgem *et al.* (2006)
SW Iberian Mediterranean S/M						
	ALCO	I. Perez-Ramos	-6	36	CC	Pérez-Ramos *et al.* (2014)
	PNLA	A. Hampe	-6	37	CC	Hampe & Bairlein (2000)
	SJDV	F. Rodriguez-Sanchez	-6	37	CC	
Taiwan subtropical evergreen forests						
	FFDF	C. Chang-Yang; I-Fang Sun	122	25	ST	
Upper Midwest forest-savanna transition						

Eco-region	Plot	PI(s)	lon	lat	ST/CC	Citation
Valdivian temperate forests						
	LNP	J. Sanguinetti; T. Kitzberger	-71	-39	CC	Sanguinetti & Kitzberger (2008
	ARAU	M. Aravena; S. Donoso Calderon	-71	-38	CC	
W European broadleaf forests						
W Great Lakes forests						
	CADI	R. Kobe	-86	44	ST CC	
	MANI	R. Kobe	-86	44	ST CC	
	MICH	J. LaMontagne	-88	47	CC	
	PAFA	J. LaMontagne	-90	46	CC	
	TREE	J. S. Clark	-90	45	ST CC	
	UMBS	I. Ibanez	-85	46	ST	
	UNDE	J. S. Clark	-90	46	ST CC	
	WILW	J. LaMontagne	-90	46	CC	
	WORU	J. LaMontagne	-90	46	CC	
W Gulf coastal grasslands						
W short grasslands						
	CMNM	M. Redmond	-104	37	CC	Redmond *et al.* (2012)
	KENT	M. Redmond	-103	37	CC	Redmond *et al.* (2012)
Willamette Valley forests						
	CAMT	J. Franklin	-123	45	CC	
Wyoming Basin shrub steppe						
	NORT	A. Wion; M. Redmond	-109	41	CC	

Table S3: Origin of maximum diameter (d_{max}), with the number of species for each data source retained for the analysis used in this study.

Data source of d_{max}	Nb of species	Comments
National Forest Inventories	38	Used near maximum diameter forest inventory and analysis in the United States (Gray *et al.*, 2012); forest inventory in Europe (Kunstler *et al.*, 2021); tree census data in Japan (Ishihara *et al.*, 2011).
Unpublished field tropical measurements	222	Maximum diameter value observed from French Guyana (33 species) and from Panama (189 species).
Allometric equation	12	Maximum trait height (Liu *et al.*, 2019; Carmona *et al.*, 2021) and allometric equation from pan-tropical for Africa region, South America equation for South America region and Asia equation for Asia region.
MASTIF inventories	41	Used tree size observations and near maximum diameter for species with > 90 individual unique diameter.
Online open sources	173	Wikipedia, https://www.wikipedia.org/; American conifers society, https://conifersociety.org/; Monumental trees https://www.monumentaltrees.com/en/; iPlantz, https://www.iplantz.com/, Useful tropical plants, https://tropical.theferns.info/)

Table S4: Summary of all fitted linear models between maturation size (d_{mat}) and maximum size (d_{max}) in $\log_{10}$-$\log_{10}$ testing alternative effects of climatic variables. The mean value of estimates with a confidence interval of 95%, and their p-values (p) are reported. All models have the initial structure $\log_{10}(d_{mat_s}) = \alpha + \beta_d \times \log_{10}(d_{max_s})$ represented here by the ellipse (...). Other parameters included are temperature (T) and deficit (D).

Parameters	Estimate	2.5%	97.5%	p	AIC
$...+\beta_T \times T + \beta_{dT} \times T \times \log_{10}(d_{max_s})$					
α	3.7100	1.94000	7.0700	< 0.001	-62.84
β_d	0.3050	0.15100	0.4590	< 0.001	
β_T	-0.0233	-0.03520	-0.0114	< 0.001	
β_{dT}	0.0126	0.00586	0.0193	< 0.001	
$...+\beta_D \times D + \beta_{dD} \times D \times \log_{10}(d_{max}) + \beta_T \times T + \beta_{dT} \times T \times \log_{10}(d_{max_s})$					
α	4.15e+00	1.99e+00	8.65e+00	< 0.001	-59.29
β_d	2.81e-01	1.09e-01	4.53e-01	< 0.001	
β_T	-2.43e-02	-3.66e-02	-1.20e-02	< 0.001	
β_D	2.73e-05	-7.98e-05	1.34e-04	0.617000	
β_{dT}	1.31e-02	6.18e-03	2.00e-02	< 0.001	
β_{dD}	-1.29e-05	-7.62e-05	5.03e-05	0.688000	
...					
α	1.080	0.929	1.250	0.325	-52
β_d	0.592	0.552	0.631	< 0.001	
$...+\beta_D \times D + \beta_{dD} \times D \times \log_{10}(d_{max})$					
α	1.06e+00	8.17e-01	1.38e+00	0.657	-48.12
β_d	5.93e-01	5.27e-01	6.59e-01	< 0.001	
β_D	-6.10e-06	-1.13e-04	1.01e-04	0.910	
β_{dD}	1.40e-06	-6.18e-05	6.47e-05	0.964	
$...+\beta_D \times D + \beta_T \times T$					
α	1.19e+00	9.32e-01	1.51e+00	0.165	-49.48
β_d	5.83e-01	5.42e-01	6.25e-01	< 0.001	
β_D	-3.90e-06	-2.53e-05	1.75e-05	0.721	
β_T	-1.59e-03	-4.29e-03	1.10e-03	0.246	
$...+\beta_D \times D$					
α	1.07e+00	9.09e-01	1.25e+00	0.433	-50.12
β_d	5.92e-01	5.53e-01	6.31e-01	< 0.001	
β_D	-3.70e-06	-2.52e-05	1.77e-05	0.732	
$...+\beta_T \times T$					
α	1.20000	0.94800	1.52000	0.129	-51.35
β_d	0.58300	0.54100	0.62500	< 0.001	
β_T	-0.00159	-0.00429	0.00111	0.248	
$\alpha + 1 \times \beta_d$					
α	0.244	0.232	0.257	0	248.1
β_d	1	-	-	-	
α					
α	9.25	8.69	9.85	0	447.83
β_d	0	-	-	-	

44

Table S5: Summary of the best joint trait model. The best model has been selected based on the lowest DIC value (Table S7). Traits have been included as responses (d_{max}, d_{mat}, SLA, Wood density, seed size, and species seed productivity), with temperature (T), deficit (D), and their interaction ($T : D$) as predictors, with genus as a random effect. For each response, estimate, standard error (SE), and credible interval (95%) with significance are reported (CI does not overlap 0).

Climate variable	Estimate	SE	2.5%	97.5%	*significance*
d_{max}					
T	-0.230	0.068	-0.360	-0.097	*
D	0.150	0.050	0.054	0.250	*
T:D	-0.096	0.065	-0.220	0.031	
d_{mat}					
T	-0.190	0.065	-0.320	-0.064	*
D	0.077	0.049	-0.018	0.170	
T:D	0.010	0.064	-0.110	0.140	
SLA					
T	-0.006	0.073	-0.150	0.140	
D	0.190	0.051	0.083	0.280	*
T:D	-0.047	0.065	-0.180	0.079	
Wood density					
T	0.160	0.067	0.030	0.300	*
D	0.064	0.050	-0.033	0.160	
T:D	0.019	0.064	-0.110	0.150	
Seed size					
T	0.046	0.071	-0.093	0.180	
D	-0.180	0.050	-0.270	-0.078	*
T:D	-0.075	0.064	-0.200	0.054	
Seed productivity					
T	-0.130	0.061	-0.250	-0.012	*
D	-0.061	0.048	-0.150	0.032	
T:D	-0.037	0.064	-0.160	0.085	

Table S6: Summary of conditional parameters for the effect on d_{mat} from the GJAM joint trait model. Conditioning was done on SLA, wood density, species seed productivity, seed size, and d_{max}. Standardized coefficient values are coming from matrix **A**, for direct trait effect, and **C**, for direct climate effect.

Conditional variable	Estimate	SE	2.5%	97.5%	significance
Traits					
d_{max}	0.5460	0.0266	0.4940	0.5960	*
SLA	-0.0569	0.0576	-0.1720	0.0552	
Wood density	-0.1300	0.0856	-0.3020	0.0384	
Seed size	0.0403	0.0120	0.0169	0.0639	*
Seed productivity	-0.0385	0.0100	-0.0574	-0.0180	*
Climate					
Intercept	8.36e-01	2.69e-01	3.22e-01	1.36e+00	*
T	4.11e-03	4.66e-03	-4.93e-03	1.33e-02	
D	-1.59e-04	9.53e-05	-3.49e-04	3.28e-05	
T:D	8.30e-06	4.60e-06	-8.00e-07	1.73e-05	

Table S7: Joint traits model selection (based on the lowest DIC values). GJAM models ran with different combinations of climate covariates (T, temperature, and D, deficit).

Climatic predictors in GJAM	DIC
T × D	20,575
T + D	20,603
T	20,661
D	20,898
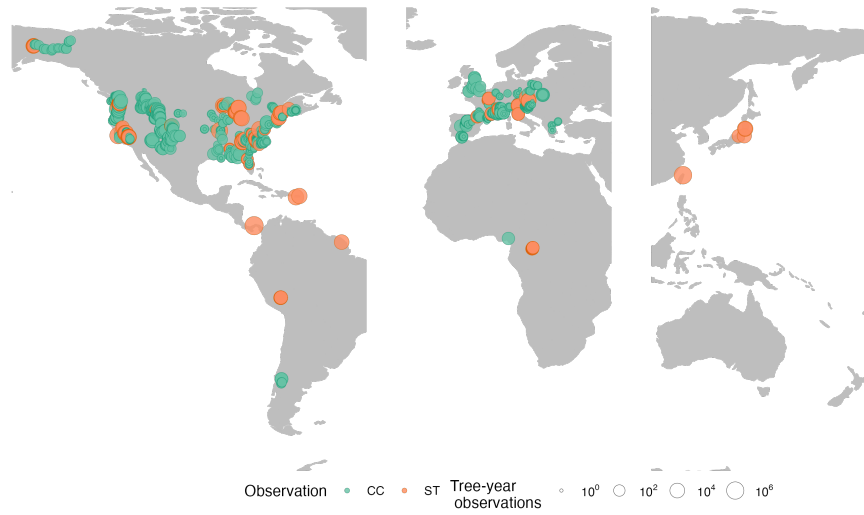
Figure S1: MASTIF data network, including seed traps data and crop count data limited here to species-genus used. The dot size represents the number of initial tree-year observations at the log10 scale. Crop count data (green dots, CC) includes 137,484 tree years observations and seed traps (orange dots, ST) 10,914,392 observations in total.
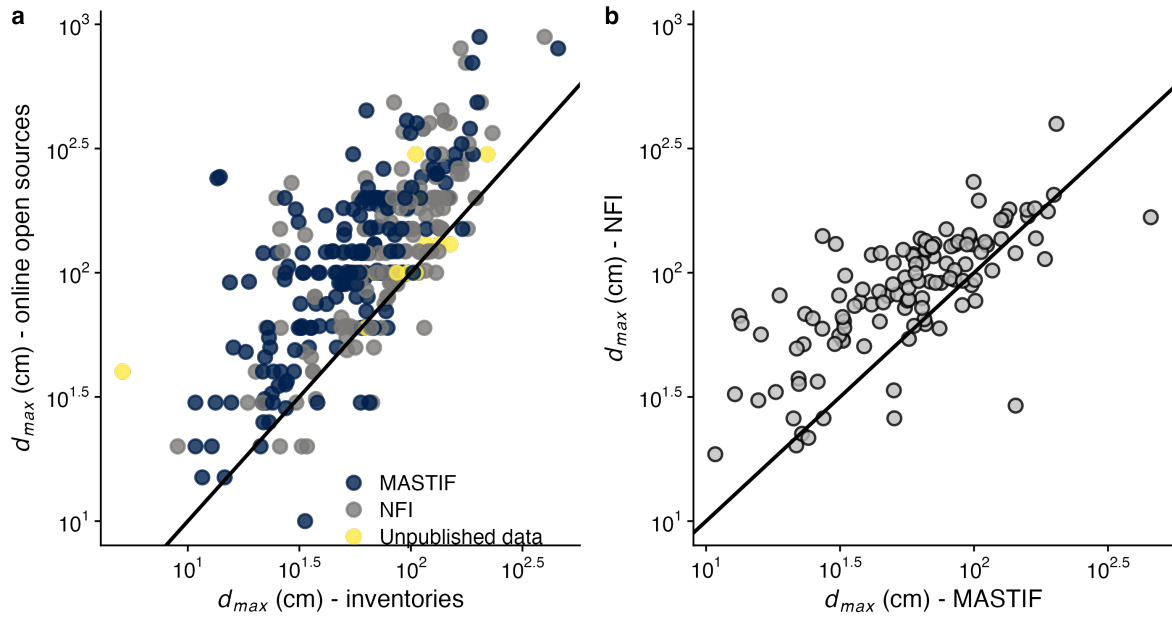
Figure S2: a) Comparison of d_{max} obtained from online open sources to d_{max} obtained from National Forest Inventories (NFI), MASTIF inventories, and from the unpublished dataset (n=191 species). b) Comparison of d_{max} obtained from National Forest Inventories (NFI) to d_{max} obtained from MASTIF inventories (N = 118 species). For both panels, the black line is the 1:1 relationship.
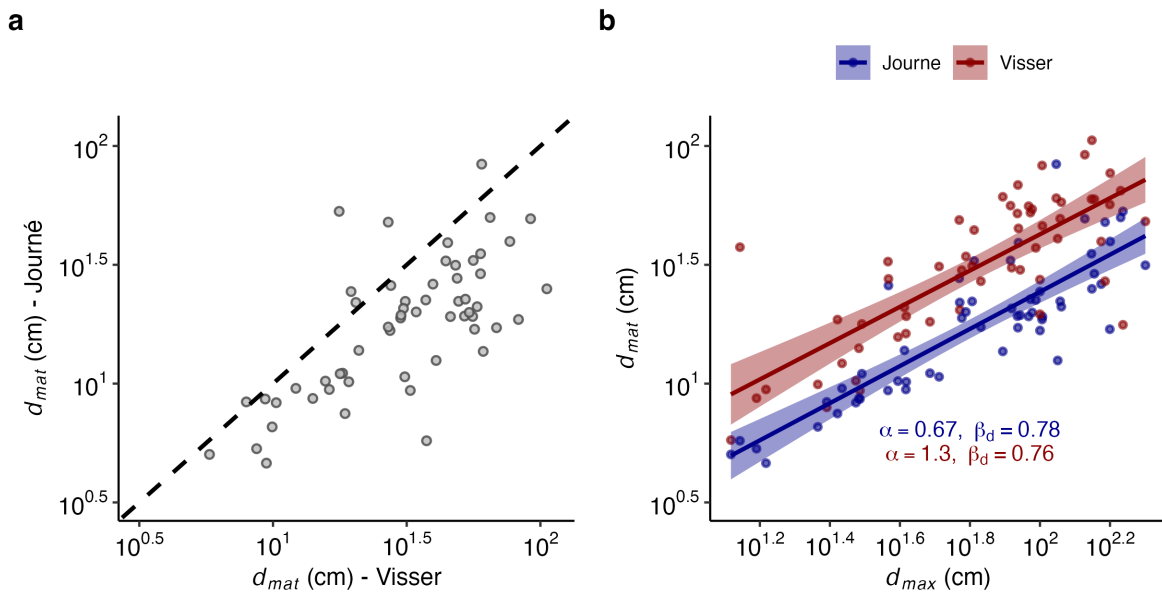
Figure S3: a) Comparison of maturation size (d_{mat}) from the main analysis (probability to produce the first fruiting structure) to maturation size (probability to reproduce at 50%) based on the reference in Visser *et al.* (2016), restricted to Barro Colorado Island, Panama. Each dot represents a single species, with the black dotted line indicating a 1:1 relationship (N = 56 species). b) Relationship between d_{mat} and d_{max} restricted to species used by Visser *et al.* (2016). The model fitted between d_{mat} and d_{max} is shown in blue for the model based on our estimates of d_{mat} and in red for estimates of d_{mat} from Visser *et al.* (2016). The regressions are reported with a confidence interval of 0.95. The average parameters α and β_d are reported for both models.
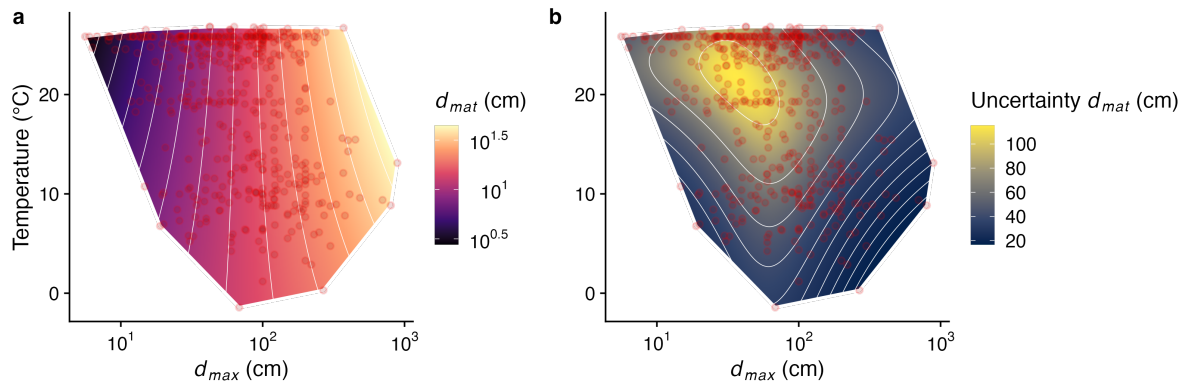
Figure S4: a) Maturation size response to d_{max} and temperature and b) Uncertainty of maturation size. Convex hulls are defined by observations (red), including the 486 tree species. In b) the surface scale color decreases as the inverse of the predictive standard error–blue edges reflect increased uncertainty at data extremes.
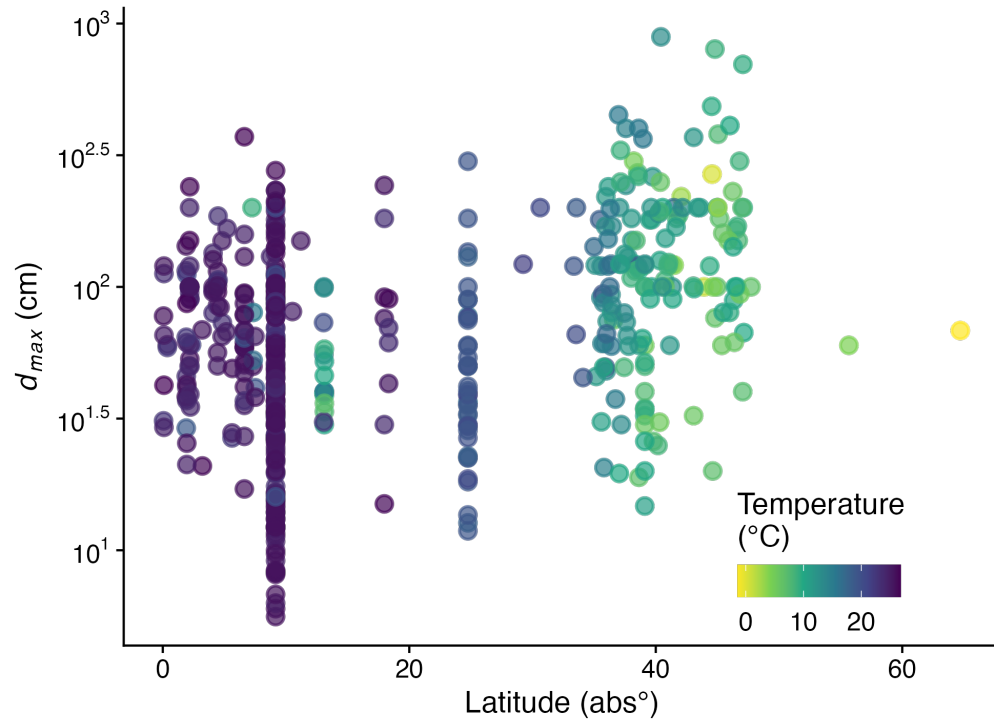
Figure S5: Relationship between d_{max} with latitude (in absolute degree) accross species. The color gradient represents the average temperature (in °C). The average latitude for each species was determined by using MASTIF inventories. Each dot represents one species.
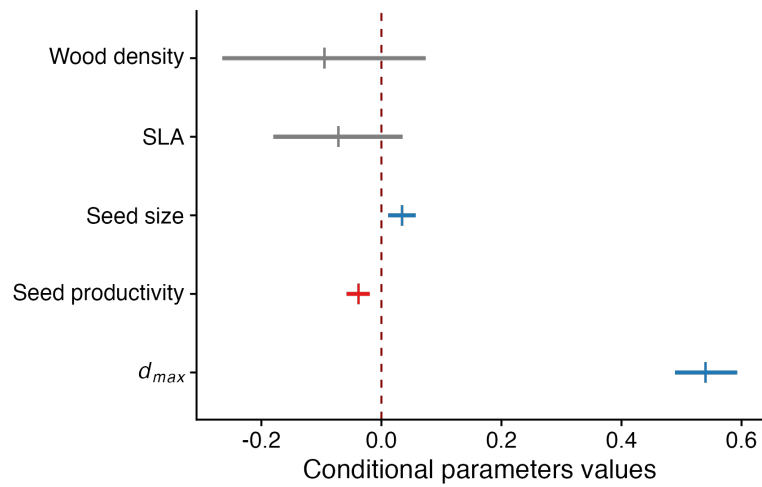
Figure S6: Conditional parameter estimates for the direct effect of traits on maturation size (d_{mat}), while accounting for trait covariance, climate and phylogeny. The climate used here has been extracted from the MASTIF inventories. Conditional parameters are evaluated on a standardized scale, making trait effects on d_{mat} respective to their variation in the data set. Points represent the posterior mean with their 95% credible intervals. Blue and red represent positive and negative associations where 95% of the posterior does not include zero. SLA, specific leaf area.
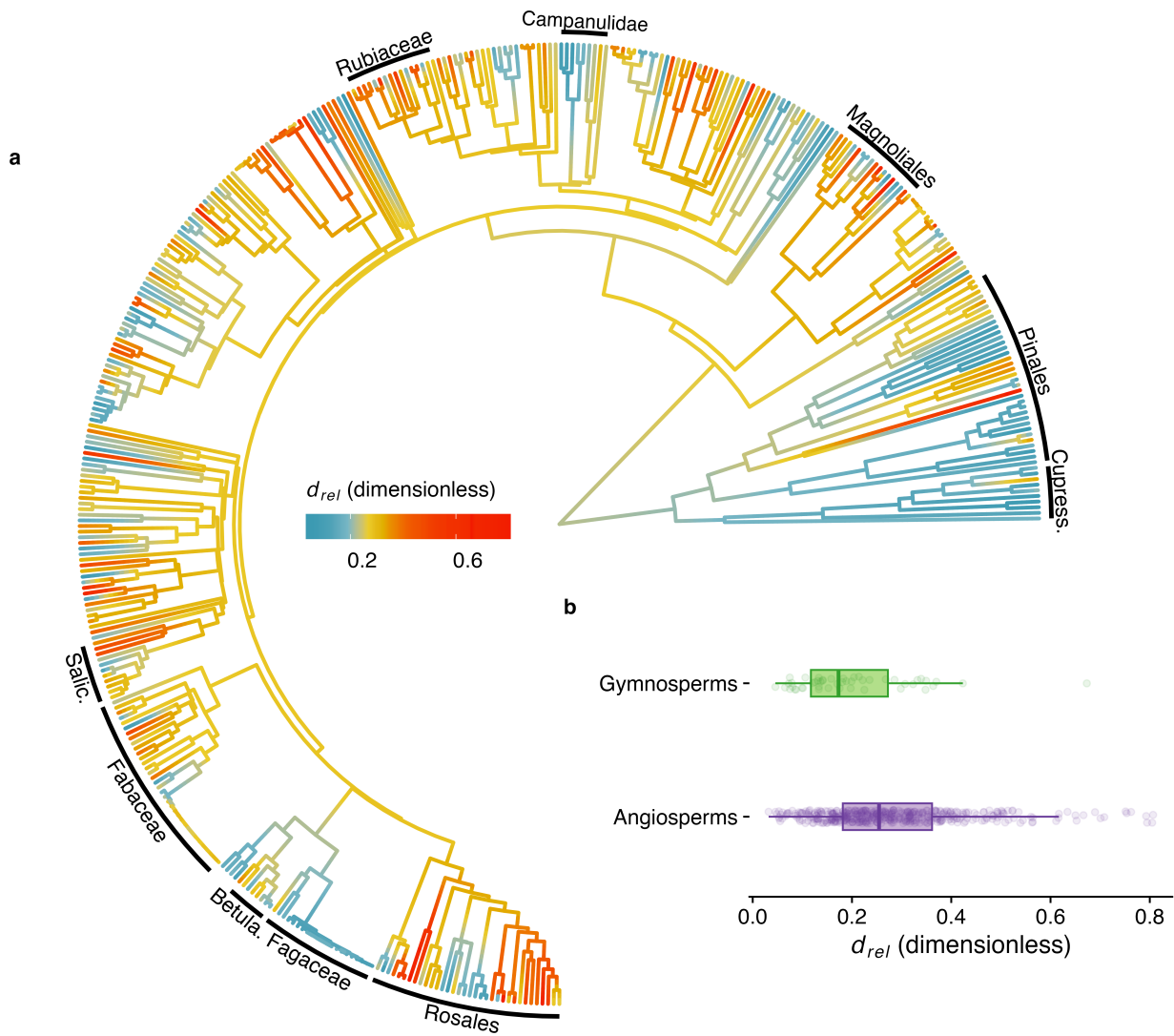
Figure S7: (a) Relative size at maturation (d_{rel}) includes a phylogenetic signal (400 species in our data have phylogenies in Zanne *et al.* 2014, Pagel's $\lambda = 0.51$, $p < 0.0001$). (b) Boxplot of relative size at maturation (d_{rel}) for gymnosperms and angiosperms (number of species is 48 for gymnosperm and 438 for angiosperm).
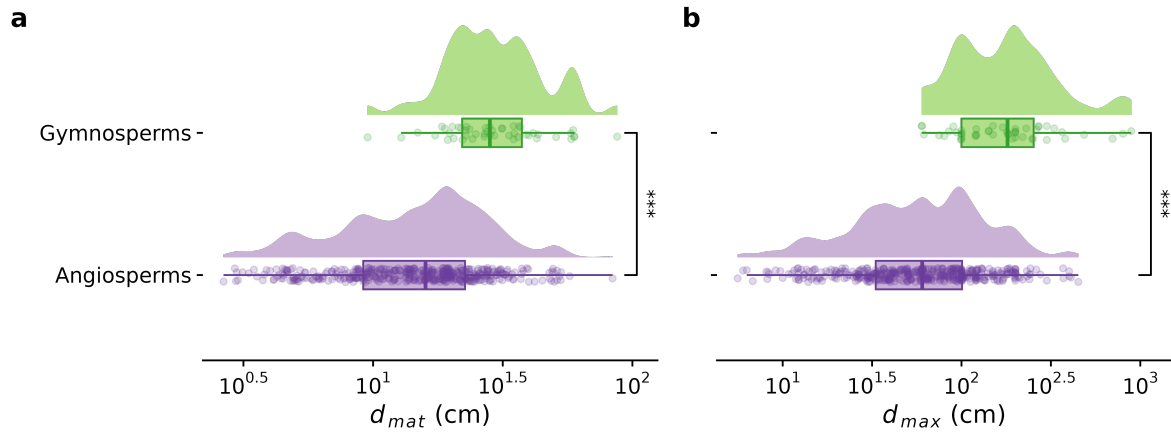
Figure S8: Boxplot of a) d_{mat} and b) d_{max} for gymnosperms (n = 48) and angiosperms (n = 438). *** indicates $p < 0.0001$ based on the sample t-test for unequal variances.
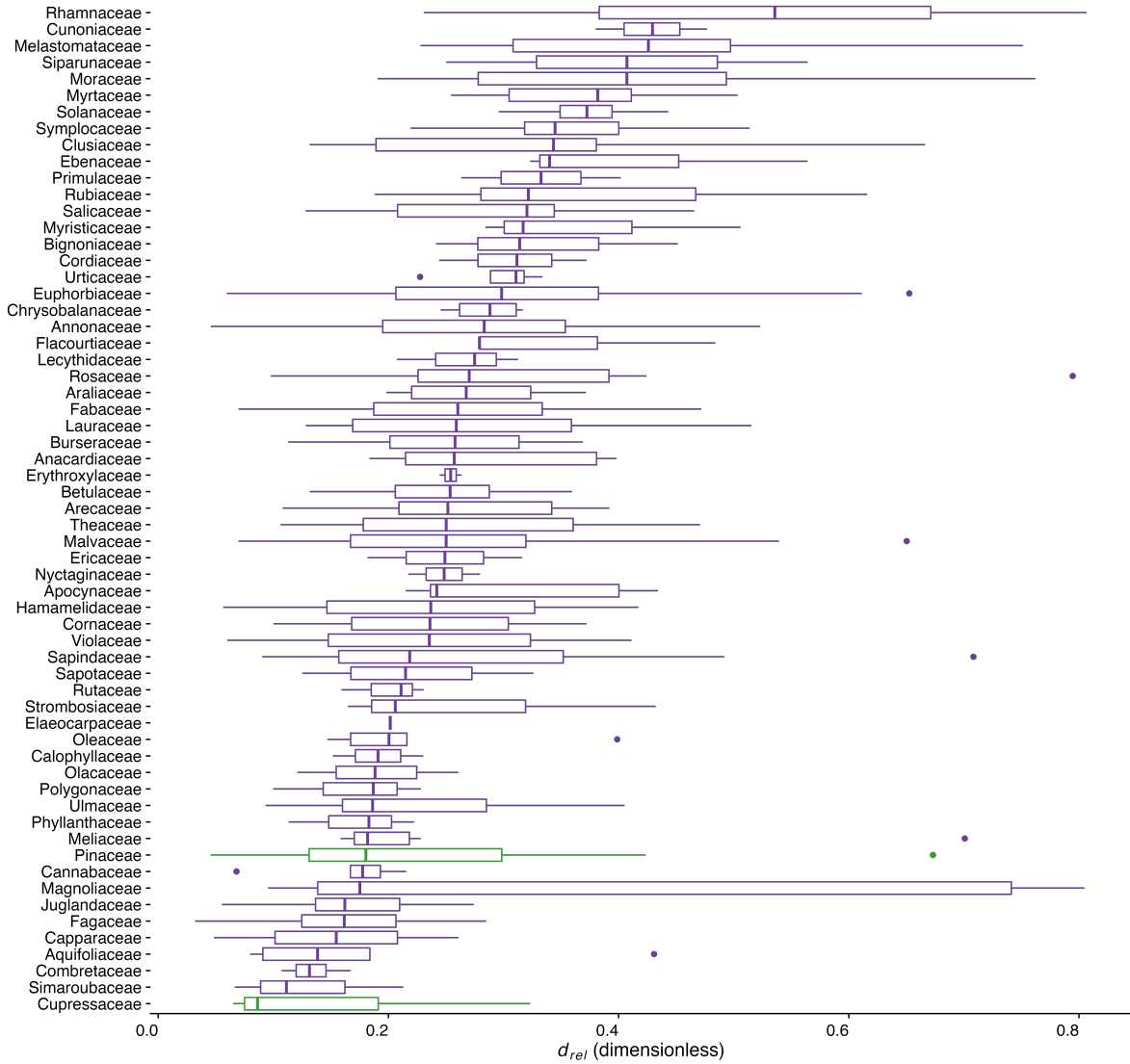
Figure S9: Boxplot of d_{rel} for families with more than one species. Green is for gymnosperms and purple for angiosperms.
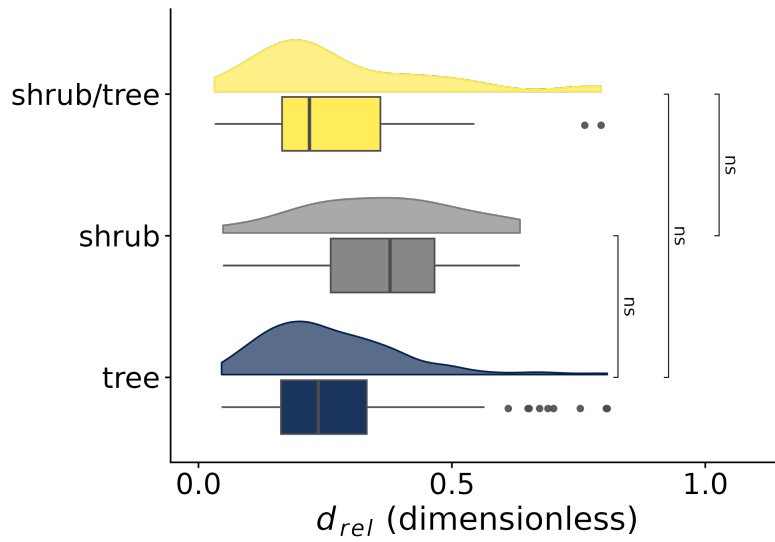
Figure S10: Boxplot with violin of variation of d_{rel} across growth forms (n = 419 species). The violin here is a mirrored density plot and showed the distribution of the data. Growth form follows a compilation from Díaz *et al.* (2022), with samples: trees, n = 361 species; shrubs, n = 17 species; shrub/tree n = 41 species. Groups were compared with a t-test for unequal variance and detected no differences according to plant growth forms (non-significant adjusted p-values with $p > 0.05$).

References supplementary material

de Andrés, E.G., Camarero, J.J., Martínez, I. & Coll, L. (2014). Uncoupled spatiotemporal patterns of seed dispersal and regeneration in pyrenean silver fir populations. *Forest Ecology and Management*, 319, 18–28.

Berdanier, A.B. & Clark, J.S. (2016). Divergent reproductive allocation trade-offs with canopy exposure across tree species in temperate forests. *Ecosphere*, 7, e01313–n/a.

Bogdziewicz, M., Acuña, M.C.A., Andrus, R., Ascoli, D., Bergeron, Y., Brveiller, D. *et al.* (2023). Linking seed size and number to trait syndromes in trees. *Global Ecology and Biogeography*, 32, 683–694.

Bogdziewicz, M., Kelly, D., Thomas, P.A., Lageard, J.G.A. & Hacket-Pain, A. (2020). Climate warming disrupts mast seeding and its fitness benefits in european beech. *Nature Plants*, 6, 88–94.

Bourg, N.A., McShea, W.J., Thompson, J.R., McGarvey, J.C. & Shen, X. (2013). Initial census, woody seedling, seed rain, and stand structure data for the scbi sigeo large forest dynamics plot. *Ecology*, 94, 2111–2112.

Caignard, T., Kremer, A., Firmat, C., Nicolas, M., Venner, S. & Delzon, S. (2017). Increasing spring temperatures favor oak seed production in temperate areas. *Scientific Reports*, 7, 8555.

Carmona, C.P., Bueno, C.G., Toussaint, A., Träger, S., Díaz, S., Moora, M. *et al.* (2021). Fine-root traits in the global spectrum of plant form and function. *Nature*, 597, 683–687.

Chen, X., Brockway, D.G. & Guo, Q. (2018). Characterizing the dynamics of cone production for longleaf pine forests in the southeastern united states. *Forest Ecology and Management*, 429, 1–6.

Clark, J.S., Bell, D.M., Kwit, M.C. & Zhu, K. (2014). Competition-interaction landscapes for the joint response of forests to climate change. *Global Change Biology*, 20, 1979–1991.

Clark, J.S., Iverson, L., Woodall, C.W., Allen, C.D., Bell, D.M., Bragg, D.C. *et al.* (2016). The impacts of increasing drought on forest dynamics, structure, and biodiversity in the united states. *Global Change Biology*, 22, 2329–52.

Clark, J.S., LaDeau, S. & Ibanez, I. (2004). Fecundity of trees and the colonization–competition hypothesis. *Ecological Monographs*, 74, 415–442.

Cleavitt, N.L. & Fahey, T.J. (2017). Seed production of sugar maple and american beech in northern hardwood forests, new hampshire, usa. *Canadian Journal of Forest Research*, 47, 985–990.

Daskalakou, E.N., Koutsovoulou, K., Ioannidis, K., Koulelis, P.P., Ganatsas, P. & Thanos, C.A. (2019). Masting and regeneration dynamics of abies cephalonica, the greek endemic silver fir. *Seed Science Research*, 29, 227–237.

864 Davi, H., Cailleret, M., Restoux, G., Amm, A., Pichot, C. & Fady, B. (2016). Disentangling the factors driving
865   tree reproduction. *Ecosphere*, 7, e01389.

866 Debain, S., Curt, T., Lepart, J. & Prevosto, B. (2003). Reproductive variability in pinus sylvestris in southern
867   france: Implications for invasion. *Journal of Vegetation Science*, 14, 509–516.

868 Detto, M., Visser, M.D., Wright, S.J. & Pacala, S.W. (2019). Bias in the detection of negative density depen-
869   dence in plant communities. *Ecology Letters*, 22, 1923–1939.

870 Díaz, S., Kattge, J., Cornelissen, J.H., Wright, I.J., Lavorel, S., Dray, S. *et al.* (2022). The global spectrum of
871   plant form and function: enhanced species-level trait dataset. *Scientific Data*, 9, 1–18.

872 Dormont, L., Baltensweiler, W., Choquet, R. & Roques, A. (2006). Larch- and pine-feeding host races of
873   the larch bud moth (zeiraphera diniana) have cyclic and synchronous population fluctuations. *Oikos*, 115,
874   299–307.

875 Doublet, V., Gidoin, C., Lefèvre, F. & Boivin, T. (2019). Spatial and temporal patterns of a pulsed resource
876   dynamically drive the distribution of specialist herbivores. *Scientific Reports*, 9, 17787.

877 Gray, A.N., Brandeis, T.J., Shaw, J.D., McWilliams, W.H. & Miles, P. (2012). Forest inventory and analysis
878   database of the united states of america (fia). *In: Dengler, J.; Oldeland, J.; Jansen, F.; Chytry, M.; Ewald,*
879   *J., Finckh, M.; Glockler, F.; Lopez-Gonzalez, G.; Peet, RK; Schaminee, J. HJ, eds. Vegetation databases*
880   *for the 21st century. Biodiversity and Ecology. 4: 225-231.*, pp. 225–231.

881 Hacket-Pain, A., Ascoli, D., Berretti, R., Mencuccini, M., Motta, R., Nola, P. *et al.* (2019). Temperature and
882   masting control norway spruce growth, but with high individual tree variability. *Forest Ecology and Man-*
883   *agement*, 438, 142–150.

884 Hampe, A. & Bairlein, F. (2000). Modified dispersal-related traits in disjunct populations of bird-dispersed
885   frangula alnus (rhamnaceae): a result of its quaternary distribution shifts? *Ecography*, 23, 603–613.

886 Han, Q., Kabeya, D., Iio, A., Inagaki, Y. & Kakubari, Y. (2014). Nitrogen storage dynamics are affected by
887   masting events in faguscrenata. *Oecologia*, 174, 679–687.

888 Hanley, M.E., Cook, B.I. & Fenner, M. (2018). Climate variation, reproductive frequency and acorn yield in
889   english oaks. *Journal of Plant Ecology*, 12, 542–549.

890 Ishihara, M.I., Suzuki, S.N., Nakamura, M., Enoki, T., Fujiwara, A., Hiura, T. *et al.* (2011). Forest stand
891   structure, composition, and dynamics in 34 sites over japan. *Ecological Research*, 26, 1007–1008.

892 Knops, J.M.H. & Koenig, W.D. (2012). Sex allocation in california oaks: Trade-offs or resource tracking? *PLOS*
893   *ONE*, 7, e43492.

Kunstler, G., Guyennon, A., Ratcliffe, S., Rüger, N., Ruiz-Benito, P., Childs, D.Z. *et al.* (2021). Demographic performance of European tree species at their hot and cold climatic edges. *Journal of Ecology*, 109, 1041–1054.

Liu, H., Gleason, S.M., Hao, G., Hua, L., He, P., Goldstein, G. *et al.* (2019). Hydraulic traits are coordinated with maximum plant height at the global scale. *Science Advances*, 5.

van Mantgem, P.J., Stephenson, N.L. & Keeley, J.E. (2006). Forest reproduction along a climatic gradient in the sierra nevada, california. *Forest Ecology and Management*, 225, 391–399.

Messaoud, Y., Bergeron, Y. & Asselin, H. (2007). Reproductive potential of balsam fir (abies balsamea), white spruce (picea glauca), and black spruce (p. mariana) at the ecotone between mixedwood and coniferous forests in the boreal zone of western quebec. *American Journal of Botany*, 94, 746–754.

Nab, L. (2021). *mecor: Measurement Error Correction in Linear Models with a Continuous Outcome*. R package version 1.0.0.

Nab, L., van Smeden, M., Keogh, R.H. & Groenwold, R.H. (2021). Mecor: An R package for measurement error correction in linear regression models with a continuous outcome. *Computer Methods and Programs in Biomedicine*, 208, 106238.

Norghauer, J.M. & Newbery, D.M. (2015). Tree size and fecundity influence ballistic seed dispersal of two dominant mast-fruiting species in a tropical rain forest. *Forest Ecology and Management*, 338, 100–113.

Parmenter, R.R., Zlotin, R.I., Moore, D.I. & Myers, O.B. (2018). Environmental and endogenous drivers of tree mast production and synchrony in piñon–juniper–oak woodlands of new mexico. *Ecosphere*, 9, e02360.

Pérez-Ramos, I.M., Aponte, C., García, L.V., Padilla-Díaz, C.M. & Marañón, T. (2014). Why is seed production so variable among individuals? a ten-year study with oaks reveals the importance of soil environment. *PLOS ONE*, 9, e115371.

Qiu, T., Sharma, S., Woodall, C.W. & Clark, J.S. (2021). Niche Shifts From Trees to Fecundity to Recruitment That Determine Species Response to Climate Change. *Frontiers in Ecology and Evolution*, 9, 1–12.

Redmond, M.D., Forcella, F. & Barger, N.N. (2012). Declines in pinyon pine cone production associated with regional warming. *Ecosphere*, 3, art120.

Rodman, K.C., Veblen, T.T., Chapman, T.B., Rother, M.T., Wion, A.P. & Redmond, M.D. (2020). Limitations to recovery following wildfire in dry forests of southern colorado and northern new mexico, usa. *Ecological Applications*, 30, e02001.

Rose, A.K., Greenberg, C.H. & Fearer, T.M. (2012). Acorn production prediction models for five common oak species of the eastern united states. *The Journal of Wildlife Management*, 76, 750–758.

925   Sanguinetti, J. & Kitzberger, T. (2008). Patterns and mechanisms of masting in the large-seeded southern
926   hemisphere conifer araucaria araucana. *Austral Ecology*, 33, 78–87.

927   Straub, J.N., Kaminski, R.M., Leach, A.G., Ezell, A.W. & Leininger, T. (2016). Acorn yield and masting traits
928   of red oaks in the lower mississippi river alluvial valley. *Forest Science*, 62, 18–27.

929   Uriarte, M., Clark, J.S., Zimmerman, J.K., Comita, L.S., Forero-Montana, J. & Thompson, J. (2012). Multidi-
930   mensional trade-offs in species responses to disturbance: implications for diversity in a subtropical forest.
931   *Ecology*, 93, 191–205.

932   Viglas, J., Brown, C. & Johnstone, J. (2013). Age and size effects on seed productivity of northern black
933   spruce. *Canadian Journal of Forest Research-Revue Canadienne De Recherche Forestiere*, 43, 534–543.

934   Whipple, A.V., Cobb, N.S., Gehring, C.A., Mopper, S., Flores-Rentería, L. & Whitham, T.G. (2019). Long-term
935   studies reveal differential responses to climate change for trees under soil- or herbivore-related stress.
936   *Frontiers in Plant Science*, 10.

937   Wion, A.P., Weisberg, P.J., Pearse, I.S. & Redmond, M.D. (2020). Aridity drives spatiotemporal patterns of
938   masting across the latitudinal range of a dryland conifer. *Ecography*, 43, 569–580.

939   Wright, B.R. & Zuur, A.F. (2014). Seedbank dynamics after masting in mulga (acacia aptaneura): Implications
940   for post-fire regeneration. *Journal of Arid Environments*, 107, 10–17.